scientific reports

Check for updates

OPEN

Effect of nanoemulsions of *Araucaria heterophylla* and *Azadirachta indica* leaf extracts against *Culex pipiens*: biochemical impacts and phytochemical profile

Lamya Ahmed Alkeridis[1]✉, Laila Ali M. Al-shuraym[1], Hend M. Alharbi[1], Mohamed M. Baz[2,3]✉, Abdelfattah Selim[4]✉ & Esraa A. Elhawary[5]

Botanical extracts and essential oils derived from medicinal plants have attracted increasing interest as eco-friendly alternatives to synthetic insecticides for mosquito control. In the present study, nanoemulsion formulations of *Araucaria heterophylla* and *Azadirachta indica* leaf extracts were developed to enhance their insecticidal efficacy against *Culex pipiens* and their biochemical impacts. Nanoemulsions were characterized using UV–Vis spectroscopy, dynamic light scattering, zeta potential analysis, and transmission electron microscopy, confirming stable nanoscale droplets with spherical morphology. Biochemical analyses revealed significant inhibition of detoxification (acetylcholinesterase, *α*- and *β*-esterases), metabolic (GABA-T, amylase, lipase), and antioxidant enzymes (SOD, GST, CAT, GSH). Elevated lipid peroxidation and protein carbonyl levels reflected severe oxidative stress, with *A. indica* nanoemulsion inducing the most potent effects. The phytochemical profiling of the two plants leads to the identification of 28 and 42 volatile components from the AIW and AH n-hexane extracts, respectively. The identified components belonged to the alkyl benzene and hydrocarbons in common between the two plants. However, AH-Hex was rich with sesquiterpenoids and oxygenated terpenoids such as caryophyllene, humulene, *β*-bisabolene, carotol, and kaurene derivatives, while AIW-Hex showed methyl esters of palmitic and stearic acids, along with long-chain branched alkanes and alcohols, as its main components. In addition, the UPLC/MS-assisted profiling of Me, Eth. Ac., and Aq. extracts revealed a vast array of metabolites, counted as 56 and 55 for AIW and AH extracts, respectively. The AH extracts were presented with a rich diterpenoid profile together with several flavonoids, fatty acids, and phenolic acids, while the AIW extracts were particularly rich with flavonoids, followed by limonoids, cinnamic acid derivatives, and fatty acids. Overall, this study demonstrates that nanoemulsions of *A. indica* and *A. heterophylla* leaves significantly enhance larvicidal efficacy against *Cx. pipiens* through biochemical disruption and oxidative stress induction.

Keywords *Araucaria heterophylla*, *Azadirachta indica*, *Culex pipiens*, Nanoemulsion, Oxidative stress, Phytochemical profile

Araucaria is a genus of evergreen coniferous trees in the family Araucariaceae, comprising approximately nineteen species primarily confined to the Southern Hemisphere[1]. The genus is highly distributed throughout New Caledonia, New Guinea, eastern Australia, Norfolk Island, Chile, southern Brazil, and Argentina. Some species, such as *Araucaria columnaris*, *Araucaria cunninghamii*, and *Araucaria heterophylla*, have also been

[1]Department of Biology, College of Science, Princess Nourah bint Abdulrahman University, Riyadh 11671, Saudi Arabia. [2]Department of Biology, Faculty of Education and Arts, Sohar University, Sohar 311, Oman. [3]Department of Entomology, Faculty of Science, Benha University, Benha 13518, Egypt. [4]Department of Animal Medicine (Infectious Diseases), College of Veterinary Medicine, Benha University, Toukh 13736, Egypt. [5]Pharmacognosy, Faculty of Pharmacy, Ain-Shams University, Cairo 11566, Egypt. ✉email: laalkeridis@pnu.edu.sa; Mohamed.albaz@fsc.bu.edu.eg; Abdelfattah.selim@fvtm.bu.edu.eg

introduced to China and Pakistan[2]. Among these, *Araucaria heterophylla* (Salisb.) Franco, also known as the Norfolk Island pine or Christmas tree, is an evergreen ornamental conifer that grows naturally on Norfolk Island and is grown in many tropical and subtropical areas. Besides being pretty and useful for wood, *A. heterophylla* has recently been noticed as a good source of natural chemicals that can kill insects and their larvae.

Araucaria species have been recognized since antiquity for their therapeutic characteristics, including anti-inflammatory, antipyretic, anti-ulcerative, antiviral, antibacterial, neuroprotective, anticoagulant, and antidepressant effects[3–5]. Different species serve various medicinal functions; for example, the leaves of *Araucaria angustifolia* are used against respiratory infections, as an emollient, and for rheumatism. The resin of *Araucaria araucana* is applied to wounds to help cicatrization and treat ulcers. In South Africa, the bark of *Araucaria bidwillii* is used orally for treating amenorrhea, while *Araucaria cunninghamii* is utilized in rituals by the people of Yali in New Guinea. Specifically, the aerial components and leaves of *A. heterophylla* have been traditionally used to alleviate toothache[2]. Additionally, studies on the fruit have shown that it can kill larvae, reduce inflammation, lower fevers, fight parasites, and control blood.

Phytochemical studies have found different chemical compounds in various *Araucaria* species, mainly including flavonoids, sesquiterpenes, and diterpenes. *A. heterophylla* leaves and resin are full of monoterpenes, sesquiterpenes, diterpenes, phenolic acids, and flavonoids. These are all known to be neurotoxic and oxidative to insects[6]. The chloroform extract of *A. heterophylla* oleogum resin is known to contain a significant amount of labdane diterpenes, which are very effective at combating oxidation and ulcers. Additionally, the essential oil (EO) is a primary component of *Araucaria* species. The main component of the essential oil from *A. heterophylla* leaves in Australia was found to be α-pinene, while the essential oil from Indian samples includes 13-epidolabradiene. In the oleogum resin of the same plant, predominant chemicals include α-copaene, germacrene D, γ-gurjunene, and δ-cadinene. Five lignans (secoisolariciresinol, pinoresinol, eudesmin, lariciresinol, and lariciresinol-4-methyl ether) were isolated from a methanol (MeOH) extract from *Araucaria araucana* (Mol.) K. Koch wood for the first time in this species, and their structures were determined with spectroscopic methods. At present, there are few studies on the composition of the essential oil from the oleogum resin of *A. heterophylla* sourced from Egyptian culture.

Azadirachta indica A. Juss., commonly known as the neem tree, belongs to the family Meliaceae and is widely distributed throughout tropical and subtropical regions[7]. It is an omnipotent tree, also known as Pokok Mambu in Malaysia, and is considered endemic to Africa, Australia, and Southern Asia, with a particularly wide distribution in India and Malaysia[8,9]. For centuries, neem has been valued for its extensive medicinal, agricultural, and ecological applications, particularly for its role as a natural insecticide[10,11]. People have used this plant in traditional medicine since prehistoric times. The leaves are used to treat malaria, fever, sore throats, and skin infections, while the fruit is used to treat sores and body pain and to keep bugs away. Additionally, the stem bark and leaf are employed in the treatment of inflammation, diabetes, and bronchitis[8,9]. Today, *A. indica* is also used in different industries, like making polyurethane coatings, creating biodiesel instead of using petroleum, and packaging seed oil for nanoemulsions.

Research has shown that *A. indica* has strong effects against larvae, reduces inflammation, lowers fever, fights parasites, and helps with diabetes. The plant has many beneficial compounds like azadirachtin, salannin, nimbin, nimbidin, and gedunin, which are very effective at killing insects and keeping them away. Azadirachtin, the main active ingredient, is known to mess with the hormones that control insect growth, stop the molting process, and affect reproduction. Many studies have shown that *A. indica* extracts and essential oils are very effective against different types of mosquito larvae, such as *Culex pipiens*, *Aedes aegypti*, and *Anopheles stephensi*. Additionally, turning neem oil into nanoemulsion formulations has been found to increase its toxicity and lasting effectiveness by improving how well it dissolves, stays stable, and gets through the outer layer of the larvae.

Botanical insecticides derived from essential oils, flavonoids, alkaloids, and other phytochemicals have shown promising larvicidal, repellent, and growth-inhibiting effects[12]. These natural products are biodegradable, less toxic to non-target organisms, and highly compatible with integrated pest management approaches. In light of increasing environmental pollution and the escalating phenomenon of insect resistance to synthetic chemical insecticides, the shift toward such eco-friendly botanical solutions has become an urgent necessity. Relying too much on synthetic compounds has harmed ecosystems and hasn't solved the problem of controlling disease-carrying insects, which has caused these pests to multiply and spread diseases more.

Among these pests, mosquitoes, particularly *Culex pipiens*, remain a primary global threat, serving as a major vector for various pathogens[13]. Effective control of mosquito populations is crucial to reducing the transmission of life-threatening diseases. Consequently, there is a growing imperative to explore and identify plants rich in bioactive compounds capable of resisting pests. For instance, several plant-derived metabolites have demonstrated remarkable efficacy in disrupting the physiological and biochemical processes of larvae[14]. This search for potent botanical sources led to the selection of *A. heterophylla* and *A. indica* for the present study.

These plants are known for their wide range of biological activities, in addition to their ability to kill insects. Pharmacological research has demonstrated that the active compounds in these plants, similar to those in *A. indica* and various *Araucaria* species, exhibit potent antimicrobial properties, anti-inflammatory effects, and antioxidant activity[8]. The essential oils and phenolic compounds found in these plants have been effective against different types of microbes, indicating that they can provide a strong defense that may be useful for controlling pests.

However, their instability and volatility under field conditions often limit their practical application[12]. Therefore, the present study aims to evaluate the larvicidal efficacy of several *A. heterophylla* and *A. indica* extracts and their corresponding nanoemulsions against *Cx. pipiens*, a major vector of the West Nile virus. Additionally, the study seeks to characterize the phytochemical profiles of these plants to identify the bioactive constituents responsible for their insecticidal activity. This integrative approach is expected to provide new insights into eco-friendly vector management and support the development of sustainable botanical nano-biopesticides.

Materials and methods

Chemicals

The following chemicals were employed for the preparation of nanoemulsions of *Azadirachta indica* (Neem) and Abies species (Christmas tree): Stearic acid, Tween 20, sodium glycolate, butanol, and decarbonated water were purchased from Alfa Aesar, Germany. All of these reagents were obtained from Alfa Aesar, Germany (Fisher Scientific). Methyl alcohol was supplied by El-Gomhoria Company, Cairo, Egypt. Distilled water was prepared in-house through a two-stage high-purity distillation process. All chemicals and solvents were used as received, without further purification.

Plant materials and analysis

Plant collection

Fresh plant materials of *Araucaria heterophylla* Salisb. (family: Araucariaceae) and *Azadirachta indica* Mill. (Family: Meliaceae) were collected from open areas within the gardens of the Faculty of Agriculture, Benha University, Egypt (30°21′16″ N; 31°13′21″ E). The collection was conducted in full compliance with institutional, national, and international guidelines and regulations governing the ethical use of plant materials. Necessary permissions for sample collection were obtained from the Faculty of Agriculture authorities, Qalyubia Governorate, Egypt. The botanical identities of both species were authenticated by Dr. Trease Labib, a taxonomist at the Egyptian Ministry of Agriculture. Voucher specimens were prepared and deposited in the Herbarium of the Department of Pharmacognosy, Faculty of Pharmacy, Ain Shams University, under the reference numbers *Araucaria heterophylla* (PHG-P-AH-553) and *Azadirachta indica* (PHG-P-AI-554). According to local and institutional regulations, no formal ethical approval was required for plant collection or use in this study.

Plant extraction

After collection, the leaves of *A. heterophylla* and *A. indica* were gently washed with running tap water to remove dust and debris, air-dried in the shade at room temperature for 7–9 days immediately following collection. The dried material was subsequently reduced to a fine powder using a stainless-steel electric grinder. To safeguard the integrity and prevent moisture absorption, the resulting powder was stored in airtight containers until further use. Sequential extraction was performed using a Soxhlet apparatus. A range of compound polarities was targeted by employing four distinct solvents: *n*-hexane, ethyl acetate, methanol, and water. For each extraction batch, 45 g of the prepared powder was mixed with 200 mL of the respective solvent for 5–12 h, depending on the solvent's boiling point. Post-extraction, the liquid products were concentrated under reduced pressure using a rotary evaporator. The resulting crude extracts were transferred to dark glass vials and stored in a refrigerator at 4 °C to mitigate potential light-induced degradation and maintain stability, consistent with established protocols[12]. The yield of *A. indica* extracts: the methanolic extract showed the highest yield (7.5%), followed by the aqueous (3.8%), ethyl acetate (2.6%), and *n*-hexane (1.8%) extracts. Similarly, for *A. heterophylla*, the extraction yields were 6.5%, 2.2%, 3.4%, and 1.3% for methanol, water, ethyl acetate, and n-hexane, respectively. All solvents used were of HPLC grade (purity ≥ 99.9%) and were purchased from Sigma-Aldrich.

Preparation of nanoemulsions

Nanoemulsions of the *A. heterophylla* and *A. indica* methanol extract were synthesized using the homogenization technique outlined by Radwan, et al. [15], employing equal ratios of the plant extract and oleic acid. Specifically, 2.5 mL of the plant extract and 2.5 mL of oleic acid were combined in a 50 mL beaker (B1) and heated to 45 °C. Concurrently, in a separate beaker (B2), 10 mL of distilled water, 0.2 g of sodium glycocholate, 0.25 mL of butanol, and 3 mL of polysorbate 20 were amalgamated and agitated on a hotplate until a homogeneous mixture was achieved. The temperature of this aqueous phase was sustained at 45 °C via an infrared thermometer. The contents of both beakers were subsequently combined with continuous stirring at a consistent temperature to generate the primary emulsion. This emulsion was promptly cooled using ice-cold water to achieve a final volume of 40 mL. The resulting nanoemulsions were put into sealed amber glass vials and kept at room temperature (25 ± 2 °C) in the dark to keep them stable and protect the active ingredients from light damage. The formulations remained stable, with no observed phase separation or precipitation throughout the study period.

Characterization of plant extract nanoemulsion

Average droplet size and surface charge

The physicochemical properties of *Araucaria heterophylla* and *Azadirachta indica* extract nanoemulsions were evaluated to confirm their nanoscale characteristics and stability. The average droplet diameter, radius, and polydispersity index (PDI) were determined using the dynamic light scattering (DLS) technique at room temperature and a fixed scattering angle of 173°. The zeta potential (ζ-potential), representing the net surface charge and electrostatic stability of the nanoemulsion droplets, was measured by monitoring the frequency shift of scattered light at a 12° angle during laser beam irradiation. All DLS and ζ-potential measurements were performed using a Zetasizer Nano ZS instrument (Malvern Instruments Ltd., Malvern, UK) at the Egyptian Petroleum Research Institute (EPRI). For each analysis, approximately 5–10 mg of the nanoemulsion sample was dispersed in 10 mL of distilled water at 25 °C and homogenized for two minutes to ensure uniform distribution before measurement.

Transmission Electron Microscopy (TEM)

To visualize droplet morphology and confirm nanoscale structure, high-resolution transmission electron microscopy (HR-TEM; JEOL JEM-2100-115, Tokyo, Japan) was employed at the Central Laboratories of EPRI, Cairo. Imaging was conducted at accelerating voltages ranging from 100 to 200 kV. For sample preparation, 1 μL of the nanoemulsion was diluted with distilled water (1:200) and carefully deposited onto a 200-mesh carbon-

coated copper grid for 2 min. Excess liquid was gently removed using cellulose filter paper, followed by negative staining with 2% (w/w) phosphotungstic acid (PTA) for 10 s. The remaining stain was absorbed prior to imaging, ensuring high-contrast visualization of the droplet architecture and surface uniformity.

UV–Vis spectroscopic analysis

The UV-Vis absorption spectra of the prepared nanoemulsions were recorded using a Genway 6305 UV-Visible spectrophotometer (Japan). Measurements were performed at room temperature over a wavelength range of 200–800 nm. Double-distilled water was used as the reference blank. Spectra of the pure plant extracts, blank nanoemulsions, and final nanoemulsion formulations were recorded under the same conditions.

Mosquito larvicidal assay

Rearing of Culex pipiens

All experiments were conducted using *Culex pipiens* larvae reared under controlled laboratory conditions. The mosquito colony, maintained for more than six generations (F6), was established and sustained in the insectary section of the Department of Entomology, Faculty of Science, Benha University. Larvae were reared in enamel trays (30 × 25 × 15 cm) containing 2 L of dechlorinated tap water and fed twice daily with a mixture of powdered dog biscuits and Tetramin® fish food (1:1, w/w). The rearing environment was kept at 27 ± 2 °C, 75–80% relative humidity, and a 12:12 h light–dark photoperiod to ensure optimal larval development. Pupae were collected daily and transferred to screened mosquito cages (30 × 25 × 25 cm) for adult emergence. Adult mosquitoes were provided with an 8% sucrose solution as a carbohydrate source and maintained under the same environmental conditions as the larvae. Third-instar larvae were continuously available for experimental use throughout the study to ensure consistency in all bioassays.

Larvicidal activity

The larvicidal efficacy of *Araucaria heterophylla* and *Azadirachta indica* leaf extracts, along with their respective nanoemulsion formulations, was evaluated against the 3rd instar larvae of *Culex pipiens* under controlled laboratory conditions, following WHO[16] standard guidelines. The crude extracts (methanol, hexane, ethyl acetate, and aqueous) were prepared and dissolved in dechlorinated distilled water to create a 1% (w/v) stock solution. A minimal amount of Tween 20 (0.1 mL of 0.1%) was added as a non-ionic surfactant to facilitate dispersion, and the mixtures were homogenized using a magnetic stirrer and shaker to ensure uniform distribution. Serial concentrations of each extract and nanoemulsion (e.g., 50, 100, 250, 500, 1000, and 1500 ppm) were tested to determine dose-response relationships. For each concentration, twenty larvae were placed in glass beakers containing 250 mL of the test solution, with three replicates per treatment (total $n = 60$ larvae per concentration). Distilled water was used as a control for crude extracts, while a blank nanoemulsion (without extract) served as a control for the nano-formulations. Larval mortality was recorded at 24 and 48 h of exposure. In all experiments, the mortality rate in control treatments did not exceed 5%; otherwise, Abbott's formula was applied for correction.

Biochemical and oxidative stress analyses

To investigate the physiological and biochemical responses of *Culex pipiens* larvae to botanical treatments, the activities of key detoxification, metabolic, and oxidative stress enzymes were assessed following exposure to the LC_{50} concentrations of *Araucaria heterophylla* and *Azadirachta indica* methanolic extracts and their corresponding nanoemulsion formulations. The analyzed biomarkers included acetylcholinesterase (AChE), α-esterase (α-EST), β-esterase (β-EST), glutathione S-transferase (GST), reduced glutathione (GSH), superoxide dismutase (SOD), catalase (CAT), lipid peroxidation (LPO), and total protein carbonyl content (TPC), in addition to key metabolic enzymes, gamma-aminobutyric acid transaminase (GABA-T), amylase, and lipase, to elucidate potential disruptions in detoxification and oxidative defense pathways. Twenty-four hours post-treatment, surviving (alive) third-instar larvae treated with the LC_{50} concentrations of both crude extracts and nanoemulsions were collected. The collected larvae were immediately frozen in liquid nitrogen to preserve enzyme activity for further biochemical analysis. Approximately 0.5 g (50–70 larvae) from each replicate was suspended in 5 mL of chilled 50 mM sodium phosphate buffer (pH 7.0) and manually homogenized at 4 °C. The homogenates were centrifuged at 10,000 × g for 10 min at 4 °C, and the resulting supernatants were used for enzyme assays, while untreated larvae served as controls. AChE activity was determined following Ellman, et al.[17] using acetylthiocholine iodide and DTNB as substrates, with absorbance measured at 412 nm. Penilla, et al. [18] used α- and β-naphthyl acetate as substrates to measure the α- and β-esterase activities. The enzyme activity was then reported as µmol of product formed per minute per mg of protein. Total protein content was estimated by the Bradford method[19]. GABA-T activity was measured following Boer and Bruinvels[20], with absorbance recorded at 340 nm after 30 min of incubation. Amylase and lipase activities were determined according to Ishaaya and Swirski[21] and Itaya[22], respectively, by measuring the release of reaction products at 540 and 550 nm.

Oxidative stress biomarkers were also analyzed to assess the impact of treatments on the antioxidant defense system. SOD and CAT activities were measured following the methods of Nishikimi, et al. [23], respectively. GST activity was assayed using the method of Habig, et al. [24] by monitoring the conjugation of CDNB with GSH, while the reduced glutathione (GSH) content was estimated according to Beutler, et al. [25]. Lipid peroxidation (LPO) levels were expressed as malondialdehyde (MDA) following Ohkawa, et al. [26], and total protein carbonyl (TPC) content was quantified as described by Levine, et al. [27]. This integrated biochemical profiling allowed for the evaluation of both enzymatic inhibition and oxidative stress induction, providing a comprehensive understanding of how the methanolic and nanoemulsion formulations of *Araucaria heterophylla* and *Azadirachta indica* disrupt the detoxification and antioxidant defense mechanisms of *Cx. pipiens* larvae.

Phytochemical identification and analysis

GC/MS analysis

The *n*-hexane extracts of the *Araucaria heterophylla* and *Azadirachta indica* were injected into a gas chromatography coupled to mass spectrometry (Shimadzu GCMS-QP 2010, Kyoto, Japan) operating in EI mode at 70 eV, and mass spectrum acquisition was performed in the mass range of 35–500 amu. The instrument was equipped with an Rtx-5MS capillary column (30 m × 0.25 mm i.d. × 0.25 µm film thickness: Restek, USA). One microliter sample was injected in a split injection mode with a split ratio of 30:1. Separation was achieved using an initial oven temperature at 50 °C for 3 min (isothermal), then gradually increased to 300 °C at a rate of 5 °C/min (ramp) and kept constant at 300 °C for another 10 min (isothermal). Helium was used as a carrier gas with a flow rate set at 1.37 mL/min. Injector temperature was maintained at 280 °C. The mass unit interface temperature was set at 280 °C, and the ion source temperature was adjusted to 200 °C. Retention indices (RI) were calculated relative to a homologous series of n-alkanes (C8-C30) injected under the same GC conditions. Identification of the compounds was performed by comparing their mass spectra and retention indices with the data reported in the NIST-17 and Wiley library databases[28].

UPLC/MS analysis

The UPLC/ESI/MS analysis was performed for *Araucaria heterophylla* and *Azadirachta indica* methanol, ethyl acetate, and aqueous extracts using the method of [5–8]. UPLC/ESI/MS in both positive and negative ion acquisition modes was carried out on an XEVO TQD triple quadrupole instrument, Waters Corporation, Milford, MA 01757, U.S.A., mass spectrometer. Chromatographic separation of the sample was done by injecting 10 µl into a UPLC instrument equipped with a reverse-phase C-18 column (ACQUITY UPLC—BEH, 2.1 × 50 mm column; 1.7 µm particle size). The sample (100 μg/mL) solution was prepared using HPLC-grade methanol, filtered using a membrane disc filter (0.2 µm), degassed by sonication before injection, and then subjected to LC/ESI/MS analysis. The gradient mobile phase comprises two eluents: eluent A is H_2O acidified with 0.1% formic acid, and eluent B is MeOH acidified with 0.1% formic acid. Elution was made at a flow rate of 0.2 mL/min as follows: (10% B) from 0 to 5 min.; (30% B) from 5 to 15 min.; (70% B) from 15 to 22 min.; (90% B) from 22 to 25 min.; and (100% B) from 25 to 29 min. The analysis was accomplished using negative ion mode as follows: source temperature 150 °C, cone voltage 30 eV, capillary voltage 3 kV, desolvation temperature 440 °C, cone gas flow 50 L/h, and desolvation gas flow 900 L/h. Mass spectra were recorded in electrospray ionization (ESI) (negative and positive ion modes) (m/z 100–1000). UPLC/MS data were processed using Masslynx 4.1 software, and tentative identification was done by comparing their retention times (R_t), mass spectra, and fragmentation patterns with reported data.

Multivariate data analysis

The unsupervised principal component analysis (PCA) was performed using Unscrambler X 10.3 (CAMO SA, Oslo, Norway). A clustered heat map was built using NCSS, 12 software with Euclidean distance, and the unweighted pair group method[29,30].

Statistical analysis

All experimental data were statistically analyzed using SPSS software (version 22). Data normality and homogeneity of variance were verified prior to analysis. Results were expressed as mean ± SD, and differences among control and treated groups were evaluated using one-way ANOVA, followed by Tukey's post hoc test when significant differences were observed. All experiments were conducted with at least three replicates, and statistical significance was considered at $p < 0.05$.

Results

Characterization of *Araucaria heterophylla* and *Azadirachta indica* nanoemulsions

UV spectroscopy analysis of nanoemulsions

The UV-Vis absorption spectra for the green synthesized nanoemulsions (Fig. 1a and b) reveal the complex electronic environment of the encapsulated biogenic compounds. For the *A. heterophylla* nanoemulsion (S1), three distinct absorption regions were identified. The first peak, a high-energy peak, in the UV-C region (approximately 220 nm). The second peak is at 273 nm, and the third broad peak is at 501 nm. These peaks correspond to π to π* and n to π* transitions of phenolic and flavonoid constituents, respectively. Similarly, the *A. indica* nanoemulsion (S2) exhibited a characteristic peak at 354.5 nm, alongside the far-UV transitions. When compared to the spectra of the pure plant extracts and the blank (control) nanoemulsion, a clear bathochromic shift (red shift) and change in peak intensity were observed. This shift indicates a strong chemical interaction between the phytochemical functional groups and the emulsion interface, confirming that the plant metabolites are not merely suspended but are chemically integrated as stabilizing and capping agents within the nanostructure.

DLS analysis and size distribution

DLS analysis provides estimations of the average hydrodynamic size of the particles, which is often slightly larger than the actual physical size due to the measurement including the surrounding solvent layer. DLS analysis showed that the nanoemulsions prepared from *A. heterophylla* and *A. indica* extracts had average diameters of 262.5 nm (Fig. 2a) and 212.8 nm (Fig. 2b), respectively. These sizes fall within the expected range for liquid nanoparticles. The PDI (Variance P.I.) for the *A. heterophylla* nanoemulsion was 0.493, while for the *A. indica* nanoemulsion it was **0.267**. The lower PDI value for *A. indica* (closer to zero) indicates a more homogeneous size distribution and greater stability compared to the *A. heterophylla* emulsion. These results suggest a consistent droplet size distribution for the nanoemulsion, supporting the uniformity of the prepared droplets.

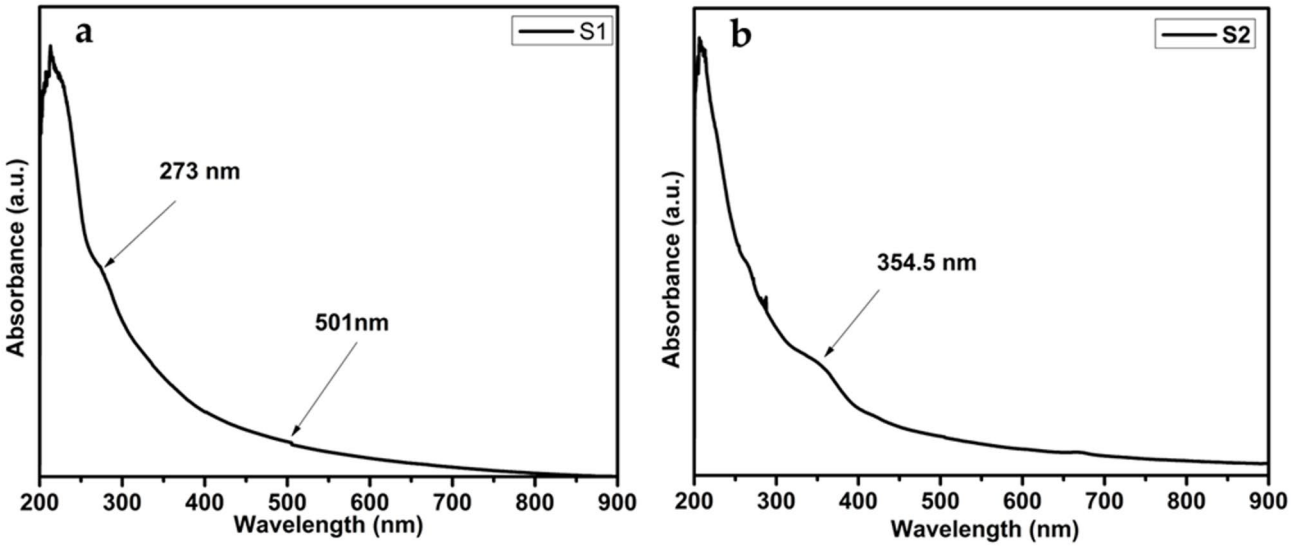

Fig. 1. Ultraviolet-visible (UV-VIS) spectroscopy of *Araucaria heterophylla* (**a**) *and Azadirachta indica* (**b**) nanoemulsion.

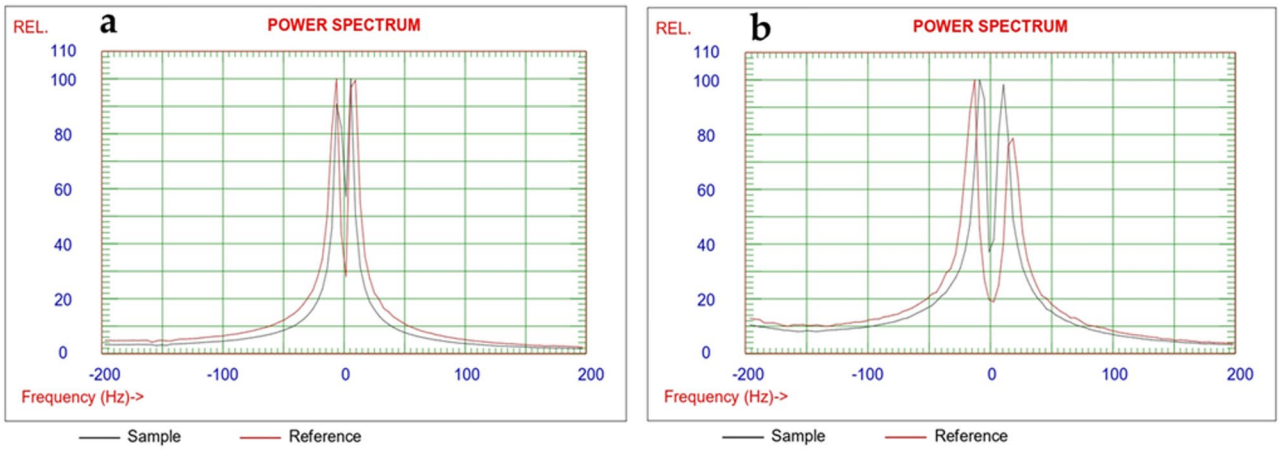

Fig. 2. Dynamic light scattering of *Araucaria heterophylla* (**a**) *and Azadirachta indica* (**b**) nanoemulsion.

Zeta potential analysis

The observed zeta potential patterns (Fig. 3a, b) confirmed the successful formation of nanoemulsions for both extracts. The *A. heterophylla* nanoemulsion (Fig. 3a) displayed two clear peaks in the power spectrum, which may suggest a mixture of particles or complex movements within the emulsion, consistent with the higher PDI value. The *A. indica* nanoemulsion (Fig. 3b) showed a more defined power peak distribution, indicating characteristic electrostatic stability, which correlates with its lower PDI value, suggesting a more uniform size distribution in the aqueous medium.

Transmission Electron Microscopy (TEM)

The TEM image (Fig. 4a) revealed nanoparticles of *A. heterophylla* with a physical width ranging from around **37.52 nm to 116.41 nm** (e.g., 37.52 nm, 95.26 nm, and 116.41 nm). This actual size is significantly smaller than the hydrodynamic size estimated by DLS (262.5 nm), confirming the phenomenon of hydrodynamic size measurement in DLS. Also, the TEM image (Fig. 4b) of *A. indica* showed well-organized nanoparticles with a width ranging from around **80 nm to 186.42 nm** (e.g., 80 nm, 80.74 nm, 136.0 nm, and 186.42 nm). The discrepancy between the DLS sizes and the TEM sizes highlights the difference between the hydrodynamic size (DLS), which includes the solvent layer and dispersion volume, and the physical/core size (TEM) of the particle in its dry state. The confirmed TEM sizes in the nano-range verify the success of the nanoemulsification technique for both botanical extracts.

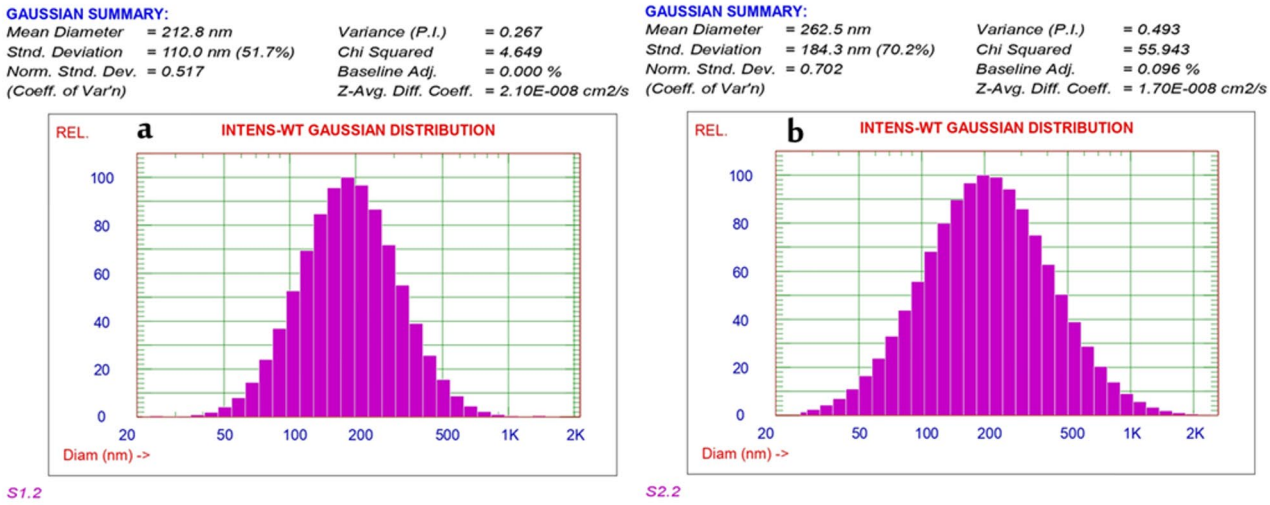

Fig. 3. Zeta potential of *Araucaria heterophylla* (**a**) *and Azadirachta indica* (**b**) nanoemulsion.

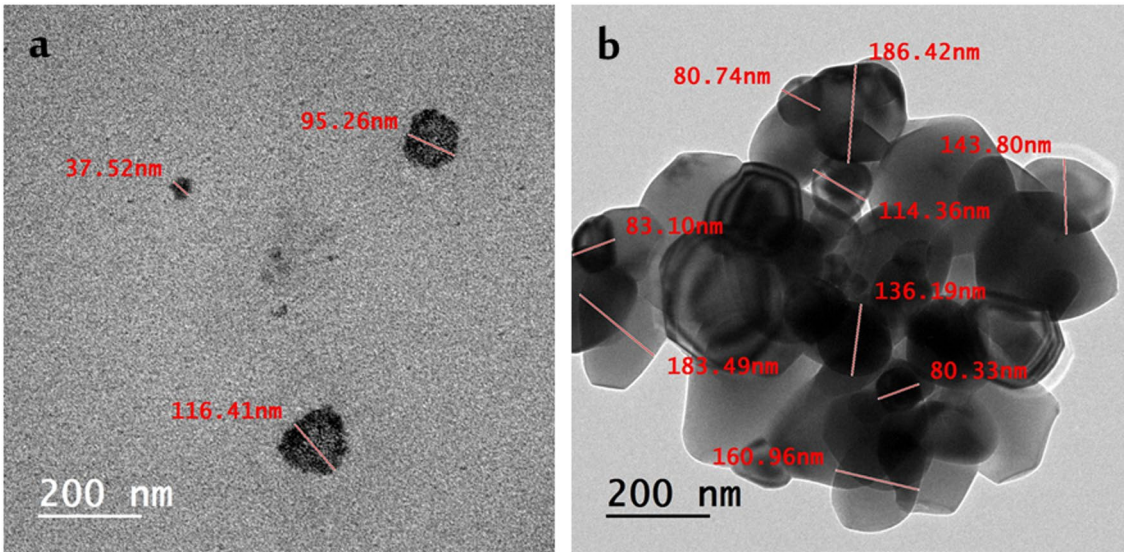

Fig. 4. Transmission Electron Microscope of *Araucaria heterophylla* (**a**) *and Azadirachta indica* (**b**) nanoemulsion.

Effects of plant nanoemulsion extracts on *Culex pipiens*

The leaf extracts of *Araucaria heterophylla* and *Azadirachta indica* exhibited marked larvicidal effects against *Culex pipiens* larvae. Data showed that *A. indica* extracts exhibited stronger larvicidal potency than *A. heterophylla*. Across all treatments, the larvicidal potency followed the order: methanol extract-nanoemulsion > methanol extract> ethyl acetate extract > hexane extract > aqueous extract. The larvicidal activity was positively correlated with both concentration and exposure time, where higher doses and longer exposure (48 h) resulted in a significant increase in larval mortality compared to lower concentrations and shorter exposure (24 h) (Tables 1, 2, 3 and 4).

The methanol extract of *A. heterophylla* exhibited the highest toxicity among the crude extracts, causing 85% mortality at 500 ppm and achieving complete larval mortality (100%) at 1000 ppm. The hexane extract produced lower mortality (65% at 500 ppm), while the aqueous extract was the least effective, causing approximately 65% mortality at the highest concentration (1000 ppm). Remarkably, the nanoemulsion formulation of *A. heterophylla* displayed the strongest insecticidal effect, inducing 100% mortality at 250 ppm within 24 h post-treatment (PT). A similar trend was recorded for *A. indica* at 24 h PT; the methanolic extract exhibited the highest toxicity among the crude extracts, causing 90% mortality at 500 ppm and achieving complete larval mortality (100%) at 1000 ppm. The hexane extract produced lower mortality (90% at 1000 ppm), while the aqueous extract was the

Plant type	Solvent	Concentration (ppm)						
		0	25	50	125	250	500	1000
Araucaria heterophylla	Methanol	0 ± 0^{aG}	5.00 ± 0.00^{bF}	11.67 ± 1.67^{bE}	26.67 ± 1.67^{bD}	46.67 ± 3.33^{bC}	85.00 ± 2.89^{bB}	100.0 ± 0.00^{aA}
	Hexane	0 ± 0^{aG}	3.33 ± 1.67^{cF}	8.33 ± 1.67^{cE}	20.00 ± 2.89^{cD}	38.33 ± 4.41^{cC}	65.00 ± 2.89^{cB}	100.0 ± 0.00^{aA}
	Ethyl acetate	0 ± 0^{aG}	1.67 ± 1.67^{dF}	6.67 ± 1.67^{dE}	16.67 ± 1.67^{dD}	35.00 ± 2.89^{dC}	60.00 ± 2.89^{dB}	85.00 ± 2.89^{bA}
	Aqueous	0 ± 0^{aG}	0.00 ± 0.00^{eF}	3.33 ± 1.67^{eE}	8.33 ± 1.67^{eD}	16.67 ± 1.67^{eC}	30.00 ± 2.89^{eB}	65.00 ± 5.00^{cA}
	Nano	0 ± 0^{aE}	11.67 ± 1.67^{aD}	23.33 ± 1.67^{aC}	60.00 ± 2.89^{aB}	100.0 ± 0.00^{aA}	100.0 ± 0.00^{aA}	100.0 ± 0.00^{aA}
	Free-Nano	0 ± 0^{aG}	3.33 ± 1.67^{cF}	8.33 ± 1.67^{cE}	10.00 ± 1.67^{eD}	15.00 ± 2.89^{eC}	21.70 ± 2.89^{fB}	$25.00 \pm 0.1.67^{dA}$
Azadirachta indica	Methanol	0 ± 0^{aG}	8.33 ± 1.67^{bF}	18.33 ± 1.67^{bE}	40.00 ± 2.89^{bD}	70.00 ± 0.00^{bC}	90.00 ± 2.89^{bB}	100.0 ± 0.00^{aA}
	Hexane	0 ± 0^{aG}	3.33 ± 1.67^{dF}	13.33 ± 1.67^{dE}	21.67 ± 1.67^{dD}	45.00 ± 2.89^{dC}	75.00 ± 2.89^{dB}	90.00 ± 5.77^{bA}
	Ethyl acetate	0 ± 0^{aG}	5.00 ± 0.00^{cF}	16.67 ± 1.67^{cE}	30.00 ± 2.89^{cD}	55.00 ± 2.89^{cC}	85.00 ± 2.89^{cB}	100.0 ± 0.00^{aA}
	Aqueous	0 ± 0^{aG}	1.67 ± 1.67^{eF}	8.33 ± 1.67^{eE}	16.67 ± 1.67^{eD}	25.00 ± 2.89^{eC}	50.00 ± 2.89^{eB}	80.00 ± 2.89^{cA}
	Nano	0 ± 0^{aD}	15.00 ± 2.89^{aC}	45.00 ± 2.89^{aB}	100.0 ± 0.00^{aA}	100.0 ± 0.00^{aA}	100.0 ± 0.00^{aA}	100.0 ± 0.00^{aA}
	Free-Nano	0 ± 0^{aG}	3.33 ± 1.67^{cF}	8.33 ± 1.67^{cE}	10.00 ± 1.67^{eD}	15.00 ± 2.89^{eC}	21.70 ± 2.89^{fB}	$25.00 \pm 0.1.67^{dA}$

Table 1. Efficacy of *Araucaria heterophylla* and *Azadirachta indica* extracts on *Culex pipiens* larval mortality, 24 h post-treatment. a, b & c: There is no significant difference ($P > 0.05$) between any two means for each plant extract, within the same column have the same superscript letter. A, B & C: There is no significant difference ($P > 0.05$) between any two means, within the same row have the same superscript letter.

Plant type	Solvent	Concentration (ppm)						
		0	25	50	125	250	500	1000
Araucaria heterophylla	Methanol	1.67 ± 1.67^{aF}	8.33 ± 1.67^{bE}	20.00 ± 2.89^{bD}	41.67 ± 1.67^{bC}	66.67 ± 1.67^{bB}	96.67 ± 3.33^{aA}	100.0 ± 0.00^{aA}
	n-Hexane	1.67 ± 1.67^{aG}	6.67 ± 1.67^{bcF}	13.33 ± 1.67^{cE}	36.67 ± 3.33^{cD}	53.33 ± 3.33^{cC}	81.67 ± 1.67^{bB}	100.0 ± 0.00^{aA}
	Ethyl acetate	1.67 ± 1.67^{aG}	3.33 ± 1.67^{cdF}	10.00 ± 0.00^{cdE}	20.00 ± 0.00^{dD}	43.33 ± 3.33^{dC}	70.00 ± 2.89^{cB}	96.67 ± 3.33^{aA}
	Aqueous	1.67 ± 1.67^{aG}	1.67 ± 0.42^{dF}	6.67 ± 1.67^{dE}	13.33 ± 3.33^{eD}	25.00 ± 2.89^{eC}	50.00 ± 2.89^{dB}	70.00 ± 2.89^{bA}
	Nano	1.67 ± 1.67^{aE}	18.33 ± 0.00^{aD}	55.00 ± 1.67^{aC}	95.00 ± 1.67^{aB}	100.0 ± 0.00^{aA}	100.0 ± 0.00^{aA}	100.0 ± 0.00^{aA}
	Free-Nano	0 ± 0^{aE}	5.00 ± 1.67^{cE}	8.33 ± 1.67^{eE}	11.67 ± 2.89^{fD}	18.33 ± 1.67^{fC}	26.67 ± 2.89^{fB}	33.33 ± 2.59^{dA}
Azadirachta indica	Methanol	1.67 ± 1.67^{aF}	13.33 ± 1.67^{bE}	30.00 ± 2.89^{bD}	60.00 ± 5.77^{bC}	90.00 ± 5.77^{bB}	100.0 ± 0.00^{aA}	100.0 ± 0.00^{aA}
	n-Hexane	1.67 ± 1.67^{aF}	8.33 ± 1.67^{cE}	20.00 ± 2.89^{cD}	41.67 ± 4.41^{dC}	60.00 ± 2.89^{dB}	96.67 ± 3.33^{aA}	100.0 ± 0.00^{aA}
	Ethyl acetate	1.67 ± 1.67^{aF}	8.33 ± 1.67^{cE}	25.00 ± 2.89^{cD}	50.00 ± 0.00^{cC}	75.00 ± 2.89^{cB}	100.0 ± 0.00^{aA}	100.0 ± 0.00^{aA}
	Aqueous	1.67 ± 1.67^{aG}	5.00 ± 2.89^{cF}	11.67 ± 1.67^{eE}	21.67 ± 1.67^{eD}	38.33 ± 1.67^{eC}	70.00 ± 2.89^{bB}	95.00 ± 2.89^{bA}
	Nano	0.0 ± 0.00^{aD}	23.33 ± 1.67^{aC}	75.00 ± 3.33^{aB}	100.0 ± 0.00^{aA}	100.0 ± 0.00^{aA}	100.0 ± 0.00^{aA}	100.0 ± 0.00^{aA}
	Free-Nano	0 ± 0^{aE}	5.00 ± 1.67^{cE}	8.33 ± 1.67^{eE}	11.67 ± 2.89^{fD}	18.33 ± 1.67^{fC}	26.67 ± 2.89^{fB}	33.33 ± 2.59^{dA}

Table 2. Efficacy of *Araucaria heterophylla* and *Azadirachta indica* extracts on *Culex pipiens* larval mortality, 48 h post-treatment. a, b & c: There is no significant difference ($P > 0.05$) between any two means for each plant extract, within the same column have the same superscript letter. A, B & C: There is no significant difference ($P > 0.05$) between any two means, within the same row have the same superscript letter.

Time (hr)	Treatment	LC_{50} (Low-Up.)	LC_{90} (Low-Up.)	LC_{95} (Low-Up.)	Slope ± SE	X^2 (sign.)
24	Methanol	197.87 (128.96–308.07)	778.79 (583.83–1670.61)	1148.42 (874.78–2762.52)	2.153 ± 0.138	18.072 (0.001)
	Hexane	287.75 (247.81–337.02)	1366.30 (1055.08–1897.85)	2124.83 (1566.19–3146.53)	1.894 ± 0.134	5.167 (0.270)
	Ethyl acetate	403.06 (341.92–484.33)	2128.64 (1559.04–3204.35)	3411.76 (2363.71–5551.50)	1.773 ± 0.137	2.470 (0.650)
	Aqueous	762.84 (621.84–987.32)	4159.47 (2743.43–7503.08)	6727.39 (4137.72–13464.24)	1.739 ± 0.164	7.070 (0.132)
	Nano	88.99 (78.35–101.72)	260.86 (211.76–344.67)	353.85 (276.68–494.24)	2.743 ± 0.237	7.767 (0.100)
48	Methanol	128.98 (95.98–172.65)	431.47 (329.53–695.69)	607.59 (457.34–1055.60)	2.443 ± 0.157	10.044 (0.039)
	Hexane	203.89 (174.62–239.52)	980.37 (753.59–1375.45)	1530.10 (1119.95–2299.25)	1.879 ± 0.141	5.218 (0.265)
	Ethyl acetate	254.91 (222.88–292.62)	971.56 (786.74–1262.99)	1419.69 (1108.26–1940.44)	2.205 ± 0.148	8.671 (0.069)
	Aqueous	568.72 (468.62–717.28)	3488.53 (2355.24–5972.90)	5833.74 (3678.12–11023.16)	1.626 ± 0.140	2.175 (0.703)
	Nano	52.87 (47.92–58.27)	112.05 (97.43–134.68)	138.63 (117.59–173.03)	3.929 ± 0.342	3.444 (0.486)

Table 3. Lethal concentrations (ppm) *Araucaria heterophylla* extracts on *Culex pipiens* mortality, 24 and 48 h post-treatment.

Time (hr)	Treatment	LC_{50} (Low-Up.)	LC_{90} (Low-Up.)	LC_{95} (Low-Up.)	Slope ± SE	X^2 (sign.)
24	Methanol	131.42 (114.53–150.58)	522.46 (428.10–666.79)	772.61 (611.00–1035.14)	2.138 ± 0.139	6.561 (0.160)
	Hexane	228.84 (141.26–387.94)	947.49 (726.48–2474.08)	1417.38 (1125.96–4293.56)	2.077 ± 0.139	21.467 (0.000)
	Ethyl acetate	178.53 (154.77–206.21)	791.41 (634.05–1041.37)	1207.04 (928.97–1677.66)	1.981 ± 0.131	6.343 (0.174)
	Aqueous	478.51 (397.87–593.21)	2958.08 (2044.13–4865.58)	4957.59 (3208.21–8952.42)	1.620 ± 0.133	7.186 (0.126)
	Nano	63.84 (57.18–71.20)	158.98 (135.86–194.43)	205.91 (171.16–262.21)	3.234 ± 0.256	7.916 (0.094)
48	Methanol	91.75 (67.78–122.20)	318.44 (242.72–517.87)	453.13 (339.61–800.18)	2.371 ± 0.161	9.526 (0.049)
	Hexane	147.36 (128.55–168.84)	583.63 (477.64–745.93)	862.15 (681.06–1156.42)	2.144 ± 0.139	8.893 (0.063)
	Ethyl acetate	121.26 (87.02–167.21)	456.04 (342.40–783.08)	663.86 (492.30–1244.00)	2.227 ± 0.145	11.017 (0.026)
	Aqueous	329.89 (281.27–392.23)	1748.73 (1305.54–2552.16)	2805.80 (1986.60–4406.94)	1.769 ± 0.131	9.035 (0.060)
	Nano	44.34 (40.03–48.88)	94.02 (81.87–113.10)	116.35 (98.72–145.72)	3.926 ± 0.363	5.065 (0.280)

Table 4. Lethal concentrations (ppm) *Azadirachta indica* extracts on *Culex pipiens* mortality, 24 and 48 h post-treatment.

Plant type	Acetylcholinesterase (AChE) (nmol ACh hydrolyzed/min/mg protein)	α-esterase (α-EST) (mmol/min/mg protein)	β-esterase (β-EST) (mmol/min/mg protein)
Control	10.74 ± 0.05^{a}	2.59 ± 0.04^{a}	3.48 ± 0.08^{a}
Araucaria heterophylla (extract)	8.36 ± 0.11^{b}	2.07 ± 0.03^{bc}	2.78 ± 0.06^{b}
Azadirachta indica (extract)	5.81 ± 0.03^{d}	1.67 ± 0.02^{c}	1.91 ± 0.01^{c}
Araucaria heterophylla (nanoemulsion)	6.79 ± 0.24^{c}	2.26 ± 0.08^{b}	1.80 ± 0.05^{c}
Azadirachta indica (nanoemulsion)	3.50 ± 0.17^{e}	1.12 ± 0.02^{d}	1.27 ± 0.09^{d}

Table 5. The effect of *Araucaria heterophylla* and *Azadirachta indica* extracts and nanoemulsions against the activities of different esterase enzymes in mosquitoes. a, b & c: There is no significant difference ($P > 0.05$) between any two means, within the same column have the same superscript letter.

least effective, causing approximately 80% mortality at 1000 ppm. The nanoemulsion again demonstrated the most potent effect, producing complete larval mortality at only 125 ppm (Table 1).

After 48 h PT, the mortality percentages further increased across all treatments, confirming the time-dependent nature of toxicity. For *A. heterophylla*, the methanol extract reached 96.67% mortality at 500 ppm, while the aqueous extract rose to 70% at 1000 ppm. The nanoemulsion maintained its superior performance, sustaining 95% mortality even at lower concentrations (125 ppm) and 100% at 250 ppm. By 48 h PT, all *A. indica* extracts exhibited enhanced efficacy; the methanol and ethyl acetate extracts achieved 100% mortality at 500 ppm, and the aqueous extract increased to approximately 95% at 1000 ppm. The nanoemulsion formulation sustained the highest toxicity level, with 100% mortality recorded at a concentration as low as 125 ppm within 48 h (Table 2).

Probit analysis confirmed the high larvicidal efficacy of plant nanoemulsions over extracts, recording the LC_{50} values with significant variations based on solvent type and exposure time. For *A. heterophylla*, the 24 h PT LC_{50} values were 88.99, 197.87, 287.75, 403.06, and 762.84 ppm for the nanoemulsion, methanol, hexane, ethyl acetate, and aqueous, respectively. After 48 h PT, the LC_{50} further dropped to 52.87 ppm, indicating time-dependent toxicity enhancement (Table 3). Similarly, *A. indica* extracts demonstrated higher LC_{50} values for crude extracts (131.42 ppm for methanol, 228.84 ppm for hexane, and 478.51 ppm for aqueous), while the nanoemulsion recorded a markedly lower LC_{50} of 63.84 ppm after 24 h, which decreased to 44.34 ppm after 48 h. These results highlight that nanoformulations significantly improved larvicidal efficacy, requiring smaller doses to achieve comparable or superior mortality to conventional extracts (Table 4).

Biochemical and oxidative stress of treated mosquito larvae

The study investigated the comparative effects of native extracts and nano-emulsions of *Araucaria heterophylla* and *Azadirachta indica* on key enzyme activities in mosquitoes. The results indicated that the nano-emulsion formulation of *A. indica* exhibits significant inhibitory effects on several enzyme systems and induces substantial oxidative stress when compared to the control group. All values were calculated from three replicates and are expressed as mean ± SE.

Treatment with the plant extracts, especially *A. indica* nano-emulsion, led to a significant decrease in the activities of the detoxification system. For the acetylcholinesterase (AChE), α-esterase (α-EST), and β-esterase (β-EST), the *A. indica* nano-emulsion produced the lowest measured activity values (3.50 ± 0.17, 1.12 ± 0.02, and 1.27 ± 0.09, respectively) and showed a significant difference compared to both the control group (10.74 ± 0.05, 2.59 ± 0.04, and 3.48 ± 0.08) and the *A. heterophylla* extract (5.81 ± 0.03, 1.67 ± 0.02, and 1.94 ± 0.01), Table 5. A similar trend was observed in nanoemulsion of *A. heterophylla* extract, which results in significant changes in the activities of AChE, α-EST, and β-EST (6.79 ± 0.24, 2.26 ± 0.08, and 1.80 ± 0.05, respectively) compared

Plant type	Gamma amino butyric acid transaminase (GABA-T) (mg/L)	Amylase (units/g tissue)	Lipase (units/g tissue)
Control	5.15 ± 0.02^{a}	21.97 ± 0.11^{a}	2.16 ± 0.02^{a}
Araucaria heterophylla (extract)	4.12 ± 0.02^{b}	17.58 ± 0.09^{b}	1.73 ± 0.02^{b}
Azadirachta indica (extract)	2.85 ± 0.04^{c}	12.88 ± 0.06^{d}	1.20 ± 0.03^{bc}
Araucaria heterophylla (nanoemulsion)	3.10 ± 0.02^{c}	15.16 ± 0.42^{c}	1.55 ± 0.03^{bc}
Azadirachta indica (nanoemulsion)	1.23 ± 0.01^{d}	9.40 ± 0.07^{e}	0.88 ± 0.02^{c}

Table 6. The effect of *Araucaria heterophylla and Azadirachta indica* extracts and nanoemulsions against the activities of infection response enzymes in mosquitoes. a, b & c: There is no significant difference ($P > 0.05$) between any two means, within the same column have the same superscript letter.

Plant extracts	SOD (units/g tissue)	G-S-T (units/g tissue)	CAT (U/mg protein/min)	GSH (µg/mg protein)	LPO (nmol/mg protein)	TPC (nmol/mg protein)
Control	2.76 ± 0.03^{a}	64.22 ± 0.68^{a}	4.15 ± 0.05^{a}	1.88 ± 0.03^{a}	3.98 ± 0.04^{e}	6.18 ± 0.03^{e}
Araucaria heterophylla (extract)	2.20 ± 0.03^{b}	51.38 ± 0.54^{b}	3.32 ± 0.04^{b}	1.50 ± 0.03^{b}	4.98 ± 0.04^{d}	7.72 ± 0.05^{d}
Azadirachta indica (extract)	1.73 ± 0.09^{c}	37.72 ± 0.48^{d}	2.24 ± 0.03^{d}	1.34 ± 0.06^{c}	7.37 ± 0.06^{b}	11.43 ± 0.06^{b}
Araucaria heterophylla (nanoemulsion)	1.76 ± 0.02^{c}	41.10 ± 0.43^{c}	2.66 ± 0.03^{c}	1.20 ± 0.02^{d}	6.23 ± 0.05^{c}	9.65 ± 0.06^{c}
Azadirachta indica (nanoemulsion)	1.06 ± 0.06^{d}	25.77 ± 0.48^{e}	1.70 ± 0.04^{e}	0.82 ± 0.01^{e}	9.78 ± 0.06a	14.51 ± 0.07^{a}

Table 7. The effect of *Araucaria heterophylla and Azadirachta indica* extracts against markers of the antioxidant defense in mosquitoes. a, b & c: There is no significant difference ($P > 0.05$) between any two means, within the same column have the same superscript letter.

to untreated larvae (10.74 ± 0.05, 2.59 ± 0.04, and 3.48 ± 0.08) and those treated with *A. heterophylla* extract (8.36 ± 0.11, 2.07 ± 0.03, and 2.78 ± 0.06, respectively).

For the infection response enzymes, including *gamma*-aminobutyric acid transaminase (GABA-T), amylase, and lipase. Data in Table 6 showed that *A. indica* nanoemulsion treatment again resulted in the lowest activity levels for all three esterases (1.23 ± 0.01, 9.40 ± 0.07, 0.88 ± 0.02), significantly lower than both the control and the native *A. indica* extract ($p < 0.05$). The study also assessed the extracts' impact on the antioxidant defense system of the mosquitoes, revealing a significant imbalance in the treated groups.

There was a significant reduction ($P < 0.05$) in the activity of key antioxidant enzymes, including superoxide dismutase (SOD), which decreased from 2.76 ± 0.03 units/g tissue in the control to 1.06 ± 0.06 units/g tissue in the *A. indica* nanoemulsion group Table 7. Similarly, glutathione S-transferase (G-S-T) and catalase (CAT) levels dropped significantly from 64.22 ± 0.68 units/g tissue and 4.15 ± 0.05 U/mg protein/min in the control to 25.77 ± 0.48 units/g tissue and 1.70 ± 0.04 U/mg protein/min, respectively, in the nanoemulsion treatment. The non-enzymatic antioxidant reduced glutathione (GSH) also showed a decline across all treatment groups compared to the control (1.88 ± 0.03 µg/mg protein), Table 6.

Conversely, markers of oxidative stress, such as Lipid Peroxidation (LPO) and Total Protein Content (TPC), exhibited a significant increase ($P < 0.05$). Specifically, LPO rose from 3.98 ± 0.04 in the control to 9.78 ± 0.06 nmol/mg protein in the *A. indica* nanoemulsion group, while TPC increased from 6.18 ± 0.03 nmol/mg to 14.51 ± 0.07 nmol/mg. Consistent with the other findings, the *A. indica* nanoemulsion treatment resulted in the most pronounced effects, causing the lowest levels of antioxidant defenses and the highest levels of LPO and TPC, highlighting its potency in inducing cellular stress in the mosquitoes.

Phytochemical profiling using GC/MS and UPLC/MS analyses for the *Araucaria heterophylla* and *Azadirachta indica* extracts

GC/MS analysis for the Azadirachta indica n-hexane extract

The *n*-hexane extract of *A. indica* was subjected to GC/MS analysis in order to reveal its volatile phytochemical profile. Twenty-eight components were identified (% (identification of 73.59%) and listed in Table 8. The identified compounds belonged mainly to alkane, alkyl benzene, and fatty acid esters, followed by sesquiterpenoids, diterpenoids, dicarboxylic acid esters, and lipid esters, as illustrated in Fig. 5. Among the major peaks are tetracontane (12.46%), eicosane (11.47%), heneicosane (6.18%), hexatriacontane (3.01%), (1-methyldecyl)-benzene (2.37%), (1-pentylhexyl)-benzene (2.22%), tetratriacontane (2.09%), (1-ethyldecyl)-benzene (2.03%), and (Z, E)-3,13-octadecadien-1-ol (1.90%).

GC/MS analysis for the Araucaria heterophylla n-hexane extract

GC/MS analysis was utilized for the identification of the volatile metabolites from *A. heterophylla n*-hexane extract. As detailed in Table 9, the % identification was recorded as 76.96%. The main identified classes were alkyl benzene, alkane/branched alkane, oxygenated sesquiterpenoids, and sesquiterpenoids, followed by diterpenoids, oxygenated diterpenoids, fatty acid esters, aliphatic alcohol, fatty alcohol, and aliphatic hydrocarbons, as illustrated in Fig. 6. Eicosane (12.80%), carotol (11.88%), (3,3-dimethyldecyl)-benzene (6.43%), β-bisabolene (4.38%), and (l-pentylhexyl)-benzene (3.28%) were listed as the major identified peaks.

No.	Component	Class	Rt (min.)	RI		% Composition	Mol. Formula	Identification method
				Cal.	Rep.			
1	4,6-dimethyl-Dodecane	Alkane	18.286	1275	–	1.58	$C_{14}H_{30}$	RI, MS
2	Heneicosane	Alkane	23.233	1454	–	6.18	$C_{21}H_{44}$	RI, MS
3	Nonadecane	Alkane	23.919	1481	–	1.57	$C_{19}H_{40}$	RI, MS
4	(1-butylhexyl)-Benzene	Alkyl benzene	24.723	1512	–	1.27	$C_{16}H_{26}$	RI, MS
5	Eicosane	Alkane	25.035	1525	–	11.47	$C_{20}H_{42}$	RI, MS
6	(1-pentylhexyl)-Benzene	Alkyl benzene	27.051	1619	1625	2.22	$C_{17}H_{28}$	RI, MS
7	(1-propyloctyl)-Benzene	Alkyl benzene	27.358	1619	1628	1.49	$C_{17}H_{28}$	RI, MS
8	(1-ethylnonyl)-Benzene	Alkyl benzene	27.839	1640	1656	1.69	$C_{17}H_{28}$	RI, MS
9	(1-methyldecyl)-Benzene	Alkyl benzene	28.677	1675	–	2.37	$C_{17}H_{28}$	RI, MS
10	(1-propylnonyl)-Benzene	Alkyl benzene	29.693	1720	1734	1.58	$C_{18}H_{30}$	RI, MS
11	(1-ethyldecyl)-Benzene	Alkyl benzene	30.165	1741	1755	2.03	$C_{18}H_{30}$	RI, MS
12	(1-methylundecyl)-Benzene	Alkyl benzene	30.988	1778	–	1.55	$C_{18}H_{30}$	RI, MS
13	(1-pentyloctyl)-Benzene	Alkyl benzene	31.494	1801	1813	1.63	$C_{19}H_{32}$	RI, MS
14	(1-ethylundecyl)-Benzene	Alkyl benzene	32.387	1843	1856	1.67	$C_{19}H_{32}$	RI, MS
15	(1,3,3-trimethylnonyl)-Benzene	Alkyl benzene	33.181	1880	–	1.79	$C_{18}H_{30}$	RI, MS
16	Hexadecanoic acid, methyl ester (Methyl palmitate)	Fatty acid methyl ester	33.472	1894	1898	1.73	$C_{17}H_{34}O_2$	RI, MS
17	3-methyl-Octadecane	Alkane	34.595	1949	–	1.25	$C_{19}H_{40}$	RI, MS
18	(*Z*, *E*)-3,13-Octadecadien-1-ol	Fatty alcohol	36.686	2055	2065	1.90	$C_{18}H_{34}O$	RI, MS
19	2-Methyltetracosane	Alkane	36.872	2064	–	1.25	$C_{25}H_{52}$	RI, MS
20	Phytol	Diterpenoid	37.215	2082	2083	1.61	$C_{20}H_{40}O$	RI, MS
21	Methyl stearate	Fatty acid methyl ester	37.432	2093	2098	1.69	$C_{19}H_{38}O_2$	RI, MS
22	Carbonic acid, decyl 2-ethylhexyl ester	Lipid ester	41.655	2470	–	1.06	$C_{19}H_{38}O_3$	RI, MS
23	2-Methylheptacosane	Alkane	42.171	2742	–	1.70	$C_{28}H_{58}$	RI, MS
24	4,8,13-Duvatriene-1,3-diol	Sesquiterpenoid	44.055	2849	–	1.99	$C_{20}H_{34}O_2$	RI, MS
25	Tetratriacontane	Alkane	45.160	2539	–	2.09	$C_{34}H_{70}$	RI, MS
26	1,3-Benzenedicarboxylic acid, *bis*-(2-ethylhexyl) ester	Dicarboxylic acid ester	47.603	2698	–	1.76	$C_{24}H_{38}O_4$	RI, MS
27	Hexatriacontane	Alkane	48.255	2327	–	3.01	$C_{36}H_{74}$	RI, MS
28	Tetracontane	Alkane	49.788	2267	–	12.46	$C_{40}H_{82}$	RI, MS
% Identification						73.59		
Alkane						42.56		
Alkyl benzene						19.29		
Fatty acid ester						3.42		
Fatty alcohol						1.90		
Sesquiterpenoid						1.99		
Diterpenoid						1.61		
Dicarboxylic acid ester						1.76		
Lipid ester						1.06		

Table 8. GC/MS identified compounds from the *n*-hexane extract of *Azadirachta indica*.

UPLC/MS analysis for the Azadirachta indica methanol, ethyl acetate and aqueous extracts

Fifty-six metabolites were tentatively identified and quantified through UPLC/MS analysis of the methanol (AIW-Me), ethyl acetate (AIW-Eth. Ac.), and aqueous extracts of *A. indica*. The tentatively identified metabolites were listed in Table 10, and an illustration of the identified phytochemical classes was represented in Fig. 7. Flavonoids represented the most abundant class of metabolites, followed by limonoids, cinnamic acid derivatives, and fatty acids. In addition, other minor classes were also detected, such as diterpenoids, tannins, triterpenoids, and others.

Flavonoids came first as the most abundant class of tentatively identified metabolites from *A. indica*. Certain aglycones were named and linked to the genus *Azadirachta*, *viz*., quercetin, apigenin, luteolin, kaempferol, naringenin, and chrysoeriol, which were detected herein, especially from the methanol and ethyl acetate extracts. Three quercetin derivatives were tentatively defined as hyperoside 6, quercetin-di-methyl-ether (2.31%, ethyl acetate extract only) 7, and quercetin-galloyl-hexoside (4.15%, methanol extract only)[31] with deprotonated peaks at *m/z* 463, *m/z* 329, and *m/z* 585 (587), respectively. Likewise, apigenin-pentoside-hexoside[28] and apigenin-feruloyl-hexoside[29] presented their peaks at *m/z* 563 and *m/z* 607 (609), respectively. Moreover, cynaroside (luteolin-hexoside)[30] and *di*-hydro-luteolin-*di*-pentoside (5.02%, ethyl acetate extract only)[32] appeared in ESI negative and positive modes at *m/z* 447 and *m/z* 551 (553), respectively.

In addition, two major naringenin derivatives were detected at *m/z* 565 (567) and *m/z* 339 (341) and were tentatively identified as naringenin derivative (5.05%, ethyl acetate extract)[33] and naringenin-hexoside

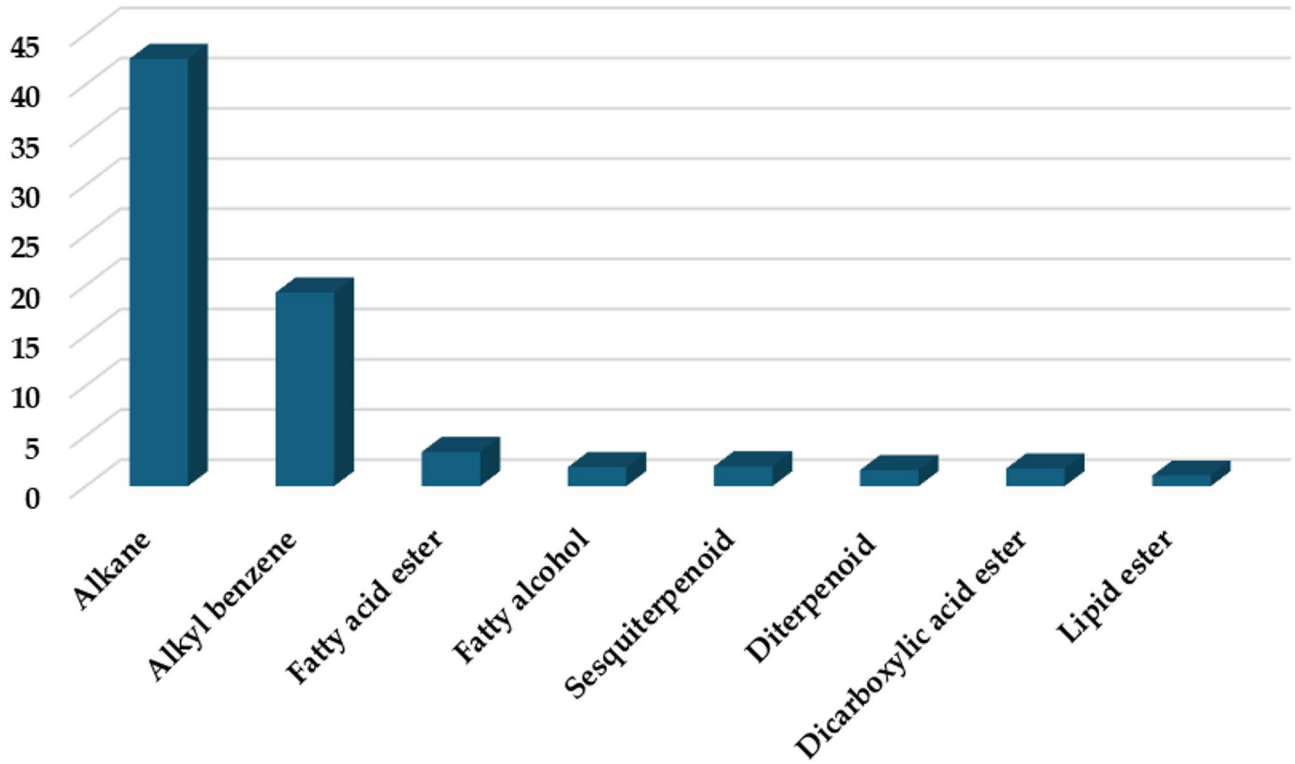

Fig. 5. The key classes of metabolites identified from *Azadirachta indican*-hexane extract.

(4.26% methanol extract and 7.98% ethyl acetate extract)[34], respectively. Other flavonoid derivatives like rutin (*m/z* 609)[35], gossypetin-hexoside (gossypin) (*m/z* 479) 15, *di*-hydro-keampferol (*m/z* 287) 16, kaempferol-deoxyhexose-pentoside (*m/z* 561)[36], kaempferol-*di*-pentoside (kaempferitrin) *(m/z* 577)[7] and chrysoeriol-hexoside (*m/z* 461)[18] were also tentatively defined and listed in Table 10.

Triterpenoids, especially limonoids, together with some diterpenoids, are regarded as characteristic metabolites of *A. indica*. Two compounds presented deprotonated peaks at *m/z* 271 and *m/z* 281 and were tentatively assigned to nimbiol[37] and lactapiperanol C 11, respectively.

Similarly, the triterpenoids *oxo*-ursa-dienoic acid[30] and oleanolic acid[38,39], together with the secotriterpenoid bruceantin[30], were also defined with their respective peaks recorded at *m/z* 451, *m/z* 455, and *m/z* 549. Several peaks were detected and defined as limonoids and listed in Table 10, such as azadirone (*m/z* 435)[37], des-acetyl-nimbinolide (*m/z* 529), *iso*-nimocinolide (*m/z* 483)[40], khayanolide A (*m/z* 515)[41], nimbandiol (*m/z* 457)[37,42], meldemin (*m/z* 455)[43], deacetyl-nimbin (*m/z* 499)[42], deacetyl-salannin (*m/z* 555), nimbionol (*m/z* 303), azadirachtol (*m/z* 581)[43], nimbocinol (*m/z* 407)[37], khayanolide B (*m/z* 517), dehydro-salannol (*m/z* 555)[43], nimbinin (*m/z* 467)[44], azadirachtanin (*m/z* 623), and *iso*-nimbolinolide (*m/z* 563)[43].

Cinnamic acid derivatives represented the third most abundant class of metabolites identified from *A. indica*. A deprotonated peak appeared at *m/z* 399 and was defined as caffeoyl quinic acid ethyl ester (1.68%, aqueous extract)[45]. Two coumaric acid derivatives were detected at *m/z* 487 and *m/z* 471 (473) and were tentatively identified as coumaric acid-*di*-hexoside[46] and *p*-coumaric acid rutinoside[47], respectively. In addition, a ferulic acid derivative[48], chlorogenic acid[35], and a quinic acid derivative[49] showed their peaks at *m/z* 517, *m/z* 353 (355), and *m/z* 441.

Short- and long-chain fatty acids were detected herein, especially from the methanol and ethyl acetate extracts of *A. indica*. The tentatively identified fatty acids were lignoceric acid[40], *oxo*-octadecadienoic acid[50], hydroxy-octadecadienoic acid[51], *di*-hydroxy-octadecadienoic acid[50], linoleic acid[52], corchorifatty acid F 11, and hexadecanoic acid (palmitic acid)[53]. Their *m/z* values, % composition, and molecular formulas were detailed in Table 10. Besides, three tannins were detected at *m/z* 331, *m/z* 635, and *m/z* 421 (423) and were tentatively defined as *mono*-galloyl-hexoside (12.06%, aqueous extract only)[54], *tri*-galloyl-hexose[55,56], and benzyl-galloyl-hexose[57], respectively.

UPLC/MS analysis for the Araucaria heterophylla methanol, ethyl acetate and aqueous extracts

Through UPLC/MS in both ESI negative and positive modes, fifty-five metabolites were tentatively identified and quantified from the methanol (AH-Me), ethyl acetate (AH-Eth. Ac.), and aqueous (AH-Aq.) extracts of *A. heterophylla*. The identified metabolites were listed in Table 11, and their respective phytochemical classes were illustrated in Fig. 8. The main identified metabolites were diterpenoids, flavonoids, fatty acids, and phenolic acids, followed by other minor classes like lignans, tannins, cinnamic acid derivatives, triterpenoids, and benzofurans.

No.	Component	Class	R_t (min.)	RI		% Composition	Mol. Formula	Identification method
				Cal.	Rep.			
1	cis-l,3-dimethyl-Cyclohexane	Aliphatic hydrocarbon	3.572	782	783	0.24	C_8H_{16}	RI, MS
2	3-Hexanol	Aliphatic alcohol	3.646	785	784	0.46	$C_6H_{14}O$	RI, MS
3	l-ethyl-3-methyl-Benzene	Alkyl benzene	7.837	938	939	1.18	C_9H_{12}	RI, MS
4	l,2,3-trimethyl-Benzene (Hemimellitene)	Alkyl benzene	8.8l5	970	976	l.08	C_9H_{12}	RI, MS
5	2-ethyl-l-Hexanol (Octyl alcohol)	Fatty alcohol	9.998	1008	1008	0.36	$C_8H_{18}O$	RI, MS
6	3-Ethyl-3-methylheptane	Branched Alkane	ll.433	1052	–	0.58	$C_{10}H_{22}$	RI, MS
7	5-methyl-Tetradecane	Branched Alkane	l7.767	1257	–	0.59	$C_{15}H_{32}$	RI, MS
8	Pentadecane	Alkane	l8.695	1289	–	0.29	$C_{15}H_{32}$	RI, MS
9	Nonadecane	Alkane	l8.9l7	1296	–	0.81	$C_{19}H_{40}$	RI, MS
10	Caryophyllene	Sesquiterpenoid	2 L.776	1399	1399	1.18	$C_{15}H_{24}$	RI, MS
11	Hexadecane	Alkane	2 L.975	1406	–	0.23	$C_{16}H_{34}$	RI, MS
12	Octadecane	Alkane	22.23 L	1416	–	0.67	$C_{18}H38$	RI, MS
13	Humulene	Sesquiterpenoid	22.655	1432	1432	0.98	$C_{15}H_{24}$	RI, MS
14	Cedr-8(15)-ene	Sesquiterpenoid	23.037	1447	1446	0.73	$C_{15}H_{24}$	RI, MS
15	2,6,l0,l5-tetramethyl-Heptadecane (Pristane)	Alkane	23.2l5	1454	–	1.24	$C_{21}H_{44}$	RI, MS
16	Heptadecane	Alkane	23.4l5	1461	–	0.35	$C_{17}H_{36}$	RI, MS
17	(-)-3,7,7-trimethyl-ll-methylene-Spiro[5.5]undec-2-ene (β-Chamigrene)	Sesquiterpenoid	23.7l5	1473	1472	0.45	$C_{15}H_{24}$	RI, MS
18	β-Bisabolene	Sesquiterpenoid	24.076	1487	1488	4.38	$C_{15}H_{24}$	RI, MS
19	Heneicosane	Alkane	24.395	1499	–	2.56	$C_{21}H_{44}$	RI, MS
20	4,6-dimethyl-Dodecane	Alkane	24.555	1505	–	0.32	$C_{14}H_{30}$	RI, MS
21	(l-butylhexyl)-Benzene	Alkyl benzene	24.7l5	1512	1526	0.91	$C_{16}H_{26}$	RI, MS
22	Eicosane	Alkane	25.035	1525	–	12.80	$C_{20}H_{42}$	RI, MS
23	Caryophyllene oxide	Oxygenated sesquiterpenoid	25.658	1550	1552	1.04	$C_{15}H_{24}O$	RI, MS
24	Carotol	Oxygenated sesquiterpenoid	26.l7l	1570	1568	11.88	$C_{15}H_{26}O$	RI, MS
25	(*E*)-l0-Heptadecen-8-ynoic acid methyl ester	Unsaturated fatty acid methyl ester	26.8l5	1596	–	0.57	$C_{18}H_{34}O_2$	RI, MS
26	(l-pentylhexyl)-Benzene	Alkyl benzene	27.055	1606	1620	3.28	$C_{17}H_{28}$	RI, MS
27	(l-propyloctyl)-Benzene	Alkyl benzene	27.353	1619	–	1.25	$C_{17}H_{28}$	RI, MS
28	(l-ethylnonyl)-Benzene	Alkyl benzene	27.833	1640	1656	1.91	$C_{17}H_{28}$	RI, MS
29	(l-methyldecyl)-Benzene	Alkyl benzene	28.672	1675	–	1.97	$C_{17}H_{28}$	RI, MS
30	(3,3-dimethyldecyl)-Benzene	Alkyl benzene	29.327	1703	–	6.43	$C_{18}H_{30}$	RI, MS
31	(l-propylnonyl)-Benzene	Alkyl benzene	29.687	1719	–	1.50	$C_{18}H_{30}$	RI, MS
32	(l-ethyldecyl)-Benzene	Alkyl benzene	30.l58	1741	1755	2.29	$C_{18}H_{30}$	RI, MS
33	(l-methylundecyl)-Benzene	Alkyl benzene	30.980	1778	1791	1.03	$C_{18}H_{30}$	RI, MS
34	(l-pentyloctyl)-Benzene	Alkyl benzene	3 L.490	1801	1813	1.74	$C_{19}H_{32}$	RI, MS
35	(l-propyldecyl)-Benzene	Alkyl benzene	3 L.897	1820	1833	0.86	$C_{19}H_{32}$	RI, MS
36	(l-methyldodecyl)-Benzene	Alkyl benzene	33.l78	1880	1894	1.53	$C_{19}H_{32}$	RI, MS
37	(8β,l3β)-Kaur-l6-ene	Diterpenoid	35.374	1987	1985	1.19	$C_{20}H_{32}$	RI, MS
38	Hexatriacontane	Alkane	36.867	2537	–	2.14	$C_{36}H_{74}$	RI, MS
39	Phytol	Oxygenated diterpenoid	37.2l5	2082	2083	0.86	$C_{20}H_{40}O$	RI, MS
40	Tetratetracontane	Alkane	42.070	1889	–	1.60	$C_{44}H_{90}$	RI, MS
41	Tritetracontane	Alkane	45.l35	2064	–	0.40	$C_{43}H_{88}$	RI, MS
Continued								
42	Tetracontane	Alkane	45.920	2587	–	1.10	$C_{40}H_{82}$	RI, MS
% Identification						76.96		
Aliphatic hydrocarbon						0.24		
Aliphatic alcohol						0.46		
Alkyl benzene						26.96		
Fatty alcohol						0.36		
Alkane/branched alkane						25.68		
Sesquiterpenoid hydrocarbon						7.72		
Oxygenated sesquiterpenoid						12.92		

No.	Component	Class	R_t (min.)	RI		% Composition	Mol. Formula	Identification method
				Cal.	Rep.			
Fatty acid ester						0.57		
Diterpenoid						1.19		
Oxygenated diterpenoid						0.86		

Table 9. GC/MS-identified metabolites from the *n*-hexane extract of *Araucaria heterophylla*.

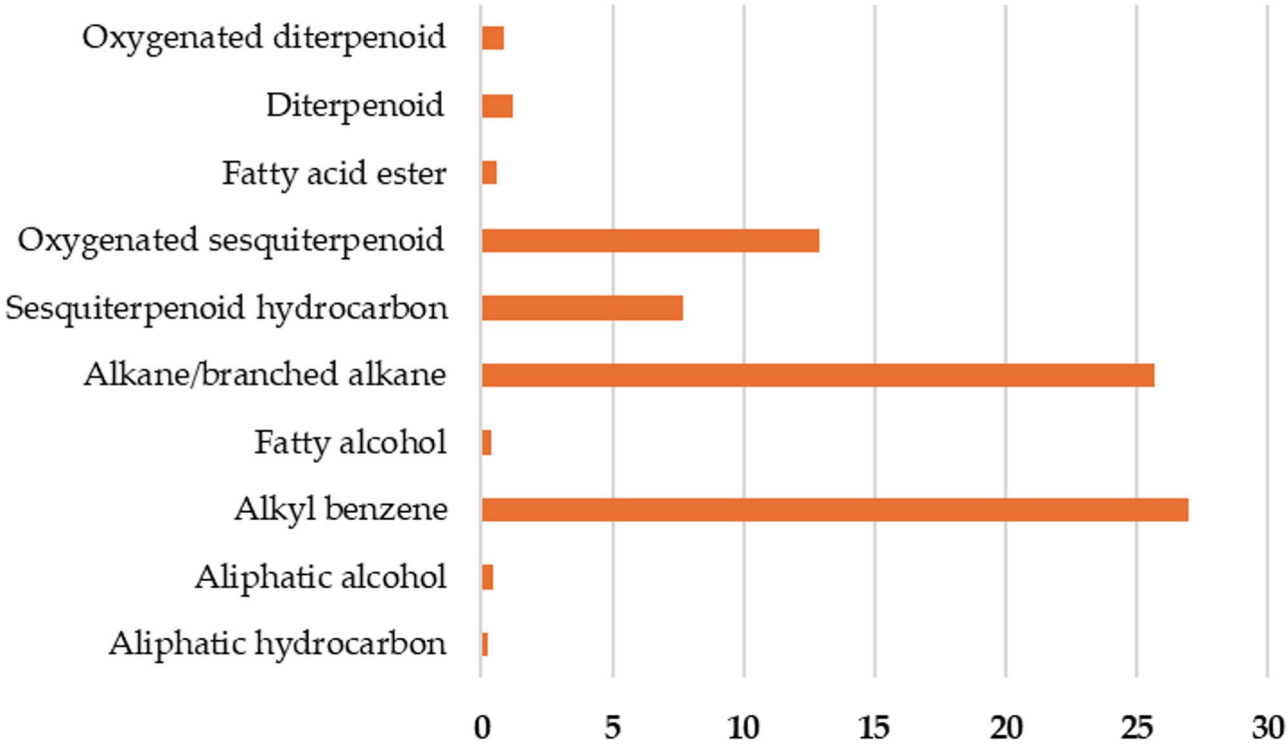

Fig. 6. The main identified classes of metabolites from *Araucaria heterophyllan*-hexane extract.

Diterpenoids

Diterpenoids represented the most abundant class of metabolites detected from the three extracts of *A. heterophylla*. Several subclasses were reported herein and matched with the documented literature about the genus *Araucaria*. The main subclasses were labdane, primarane, abietane, and clerodane. Nine labdane diterpenoids appeared as major components with high % composition and were tentatively identified as 3-keto-copalic acid (*m/z* 317) and 24-dihydro-15-acetoxy-8,9-epoxy-labdane-19-oic acid (*m/z* 377)[58], *epi*-cupressic acid (*m/z* 319)[58], acetoxy-imbricatolic acid (*m/z* 363)[59], acetyl-*epi*-cupressic acid (*m/z* 361)[58,59], *cis*/*trans*-cummunic acid (*m/z* 301)[58], 7-hydroxy-labda-8(17),13(16),14-trien-19-yl-(*E*)-coumarate (*m/z* 459)[59], labda-8(17), 14-diene (*m/z* 305)[58] and junicedric acid (*m/z* 335)[2]. Moreover, sphaeropsidin F showed a deprotonated peak at *m/z* 335 and a protonated peak at *m/z* 337, and it belonged to the primarane diterpenoid class[60] Likewise, three abietane diterpenoid peaks were detected at *m/z* 287/311, *m/z* 299, and *m/z* 287 (+ve ESI mode) and were tentatively defined as 9*β*,13*β*-epoxy-7-abietene[58], sugiol[59], and ferruginol[59], respectively.

In addition, a peak was traced at *m/z* 303/305, and it was tentatively assigned to the clerodane-type diterpenoid kolavenic acid[58]. Similarly, a trachylobane-type diterpenoid had its deprotonated peak at *m/z* 271, and it was tentatively identified as trachylobane[2].

Flavonoids were ranked as the second most abundant class of phytoconstituents identified from *A. heterophylla* extracts. An abundant deprotonated peak was detected at *m/z* 273 (6.18%, aqueous extract only), and it was tentatively defined as afzelechin[61]. Similarly, *epi*-afzelechin-hydroxybenzoate showed a deprotonated peak at *m/z* 395 (ESI +ve mode)[59]. Several other flavonoids were also identified as listed in Table 11, such as quercetin-pentoside (*m/z* 435)[62], bilobetin (*m/z* 551/553)[2], orientin (*m/z* 447)[59], methyl-retusin (*m/z* 297)[63], apigenin-hexoside (*m/z* 431)[64], chrysoeriol hexoside (*m/z* 461), and myricetin (*m/z* 317)[65]. In addition, a number of bioflavonoids, previously reported from the genus *Araucaria*, had one major peak that appeared at *m/z* 565/567 and was tentatively identified as ginkgetin[2]. Moreover, three other bioflavonoids were detected at *m/z* 551/635, *m/z* 579/581, and *m/z* 595 (+ve mode) and were assigned to *di*-methyl amentoflavone[2], *tri*-methyl-amentoflavone[2,64], and *tetra*-methylamentoflavone[1], respectively.

No.	Components	Class	Mol. Formula	R_t (min.)	$[M-H]^-$ *m/z*	$[M+H]^+$ *m/z*	% Composition			Ref.
							AIW-Me	AIW-Eth. Ac.	AIW-Aq.	
1	*tetra*-decyl-Cyclobutanoneg	Cyclic ketone	$C_{18}H_{34}O$	0.82	265	305	8.88 (10.05)	19.60	–	30
2	*oxo*-Ursa-dienoic acidg	Triterpenoid	$C_{30}H_{44}O_3$	2.27	451	–	–	–	0.58	30
3	Azadironeg	Triterpenoid (Limonoid)	$C_{28}H_{36}O_4$	5.85	435	–	0.41	–	–	87
4	Caffeoyl quinic acid ethyl ester	Cinnamic acid deriv.	$C_{18}H_{24}O_{10}$	5.88	399	–	–	–	1.68	45
5	*mono*-Galloyl-hexoside	Gallotannin	$C_{13}H_{16}O_{10}$	6.16	331	–	–	–	12.06	54
6	Ruting	Flavonoid	$C_{27}H_{30}O_{16}$	6.20	609	–	2.12	–	–	35
7	Hyperosideg	Flavonoid	$C_{21}H_{20}O_{12}$	6.42	463	–	2.02	–	–	35
8	Gossypetin-hexoside (Gossypin)	Flavonoid	$C_{21}H_{20}O_{13}$	6.60	479	–	–	–	6.70	57
9	Cynarosideg	Flavonoid	$C_{21}H_{20}O_{11}$	6.82	447	–	1.61	–	–	30
10	*di*-hydro-Luteolin-*di*-pentoside	Flavonoid	$C_{25}H_{28}O_{14}$	6.86	551	553	–	5.02	–	32
11	Stigmasterolf	Phytosterol	$C_{29}H_{48}O$	7.08	411	–	–	0.57	–	88
12	Neuraminic acid[g]	Sialic acid	$C_9H_{17}NO_8$	7.79	267	–	–	-	3.43	30
13	Coumaric acid-*di*-hexoside	Cinnamic acid deriv.	$C_{21}H_{28}O_{13}$	8.02	487	–	0.55	–	–	46
14	*tri*-Galloyl-hexose	Tannin	$C_{27}H_{24}O_{18}$	8.05	635	–	–	–	0.51	55,89
15	Ferulic acid derivative	Cinnamic acid deriv.	–	8.25	517	–	0.22	–	–	90
16	*des*-acetyl-Nimbinolideg	Triterpenoid (Limonoid)	$C_{28}H_{34}O_{10}$	9.23	529	531	2.58 (0.98)	–	–	8
17	*p*-Coumaric acid rutinoside	Cinnamic acid deriv.	$C_{21}H_{28}O_{12}$	9.49	471	473	1.83 (0.63)	–	2.52 (1.05)	47
18	Quercetin-*di*-methyl-ether	Flavonoid	$C_{17}H_{14}O_7$	9.56	329	–	–	2.31	–	91
19	Quercetin-galloyl-hexoside	Flavonoid	$C_{28}H_{24}O_{16}$	9.73	585	587	4.15 (1.53)	–	–	31
20	*di*-hydro-Keampferol	Flavonoid	$C_{15}H_{12}O_6$	9.88	287	–	–	2.11	–	92
21	*iso*-Nimocinolide[g]	Triterpenoid (Limonoid)	$C_{28}H_{36}O_7$	9.99	483	485	16.33 (3.40)	–	–	40
22	Khayanolide A[f]	Triterpenoid (Limonoid)	$C_{27}H_{32}O_{10}$	10.85	515	–	1.87	–	–	41
23	Kaempferol-deoxyhexose–pentoside	Flavonoid	$C_{26}H_{28}O_{16}$	11.11	561	–	0.59	–	–	93
24	Nimbandiolg	Triterpenoid (Limonoid)	$C_{26}H_{32}O_7$	11.14	–	457	–	–	(1.30)	42,87
25	Naringenin derivative	Flavonoid	–	12.58	565	567	–	(5.05)	–	33
26	Meldemin[g]	Triterpenoid (Limonoid)	$C_{28}H_{38}O_5$	12.85	–	455	–	–	(1.60)	43
27	deacetyl-Nimbing	Triterpenoid (Limonoid)	$C_{28}H_{34}O_8$	12.99	–	499	–	–	(0.95)	42
28	Naringenin-hexoside[g]	Flavonoid	$C_{21}H_{22}O_{10}$	13.01	339	341	4.26 (1.41)	7.98	–	34
29	deacetyl-Salannin[g]	Triterpenoid (Limonoid)	$C_{32}H_{42}O_8$	13.39	–	555	–	–	(6.29)	42
30	Lignoceric acid[g]	Long chain fatty acid	$C_{24}H_{48}O_2$	13.54	367	–	0.33	–	–	40
31	Nimbionol[g]	Triterpenoid (Limonoid)	$C_{18}H_{24}O_2$	13.78	303	–	–	0.28	–	40
32	*oxo*-Octadecadienoic acid	Fatty acid	$C_{18}H_{30}O_3$	14.66	293	317	11.09 (3.15)	11.46 (1.23)	–	94
33	Chlorogenic acid[g]	Cinnamic acid deriv.	$C_{16}H_{18}O_9$	15.23	353	355	4.55 (1.33)	2.08	–	35
34	Azadirachtol[g]	Triterpenoid (Limonoid)	–	15.28	–	581	–	(1.99)	–	43
35	Nimbocinol[g]	Triterpenoid (Limonoid)	$C_{26}H_{32}O_4$	15.60	407	409	4.25 (1.15)	–	–	87
36	Hydroxy-octadecadienoic acid	Fatty acid	$C_{18}H_{32}O_3$	15.68	295	319	–	11.43 (6.55)	–	51
37	Kaempferol-*di*-pentoside (Kaempferitrin)[f]	Flavonoid	$C_{25}H_{26}O_{14}$	16.47	577	–	0.93	–	–	91
38	Khayanolide B[f]	Triterpenoid (Limonoid)	$C_{27}H_{34}O_{10}$	16.75	517	–	2.55	–	–	41
39	dehydro-Salannol[g]	Triterpenoid (Limonoid)	$C_{32}H_{42}O_8$	17.24	555	–	6.90	–	–	43
40	Quinic acid derivative	Cinnamic acid deriv.	–	18.19	441	–	–	0.91	–	49
41	Apigenin-pentoside-hexoside	Flavonoid	$C_{27}H_{30}O_{15}$	18.33	563	–	0.22	–	–	28
42	*di*-hydroxy-Octadecadienoic acid	Fatty acid	$C_{18}H_{32}O_4$	18.78	311	–	0.70	1.62	–	94
43	Nimbiol[g]	Diterpenoid	$C_{18}H_{24}O_2$	19.04	271	–	–	0.37	–	87
44	Benzyl-galloyl-hexose	Tannin	$C_{20}H_{22}O_{10}$	19.21	421	423	2.56 (1.69)	–	–	57
45	Nimbinin[g]	Triterpenoid (Limonoid)	$C_{28}H_{34}O_6$	20.18	–	467	(2.21)	–	–	44
46	Apigenin-feruloyl-hexoside	Flavonoid	$C_{31}H_{28}O_{13}$	21.00	607	609	0.47 (6.62)	(2.83)	–	29
47	Linoleic acid[g]	Fatty acid	$C_{18}H_{32}O_2$	21.59	279	–	–	0.41	–	95
48	Hexacosanol[g]	Fatty alcohol	$C_{26}H_{54}O$	22.18	381	–	–	0.28	–	87
49	Corchorifatty acid F[g]	Fatty acid	$C_{18}H_{32}O_5$	23.10	327	407	0.83 (2.33)	1.51 (3.67)	2.08	30
50	Hexadecanoic acid (Palmitic acid)[g]	Fatty acid	$C_{16}H_{32}O_2$	23.47	255	–	0.46	0.80	0.96	96
51	Lactapiperanol C[g]	Diterpenoid	$C_{16}H_{26}O_4$	23.71	281	–	0.34	–	–	30
52	Azadirachtanin[g]	Triterpenoid (Limonoid)	C32H40O11	23.91	–	623	(9.55)	–	–	43

Continued

No.	Components	Class	Mol. Formula	R_t (min.)	$[M-H]^-$ *m/z*	$[M+H]^+$ *m/z*	% Composition			Ref.
							AIW-Me	AIW-Eth. Ac.	AIW-Aq.	
53	Chrysoeriol hexoside[g]	Flavonoid	$C_{22}H_{22}O_{11}$	26.47	461	–	–	0.31	–	97
54	Bruceantin[g]	Secotriterpenoid (quassinoid)	C28H36O11	26.91	–	549	(2.88)	–	–	30
55	*iso*-Nimbolinolide[g]	Triterpenoid (Limonoid)	C30H36O9	28.13	–	563	(0.48)	–	–	43
56	Oleanolic acid[g]	Triterpenoid	$C_{30}H_48O_3$	29.30	455	–	0.80	–	–	38,39
Number of identified components							33	22	13	
% Identification										
ESI negative mode							84.40	69.05	30.52	
ESI positive mode							49.39	21.32	11.19	

Table 10. UPLC/MS identified metabolites from *Azadirachta indica* methanol, ethyl acetate and aqueous extracts. [g] for compounds reported before from the genus *Azadirachta* and [f] for compounds reported from Family Meliaceae; AIW-Me: Neem methanol extract, AIW-Eth. Ac.: Neem ethyl acetate extract, AIW-Aq.: Neem aqueous extract; R_t: retention time.

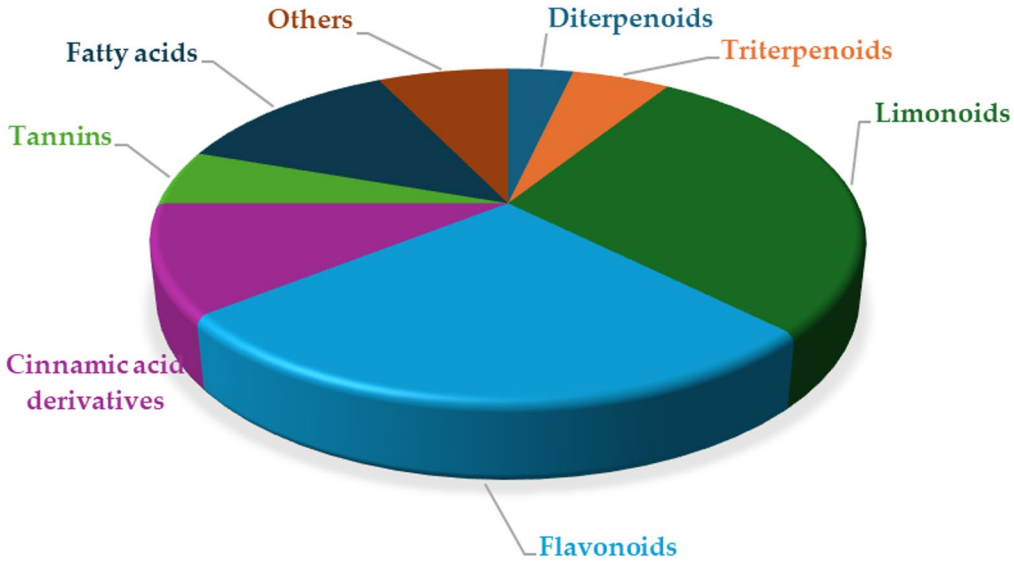

Fig. 7. The metabolites classes identified through UPLC/MS analysis of the three *Azadirachta indica* extracts.

Different peaks were tentatively defined as phenolic acids and their derivatives, viz., homovanillic acid (*m/z* 181)[59], protocatechuic acid (*m/z* 153, 9.67% AH-Me, 1.96% AH-Eth. Ac.), syringic acid (*m/z* 197)[66], syringic acid hexoside (*m/z* 359)[67], and benzoic acid derivative (*m/z* 187)[50]. In a similar fashion, one coumarin was tentatively identified as umbelliferone (*m/z* 161, aqueous extract only), a famous coumarin belonging to the genus *Araucaria*[59].

Fatty acids were well represented in the genus *Araucaria*, and herein, *Araucaria* extracts showed the presence of different fatty acids such as lauric acid (*m/z* 199)[59], linoleic acid (*m/z* 279) 35,50-*oxo*-octadecadienoic acid (*m/z* 293), 32-dihydroxy-octadecanoic acid (*m/z* 315/339)[68], hydroxy-octadecadienoic acid (*m/z* 295)[51], octadecenoic acid ethyl ester (*m/z* 309)[59], *di*-hydroxy-octadecadienoic acid (*m/z* 311)[50] and stearyl ferulate (*m/z* 445/447)[2]. In addition, several other phytoconstituents like tannins, lignans, neolignans, cinnamic acid derivatives, benzofurans, and triterpenoids were detected and listed in Table 11.

Multivariate data analysis using PCA and clustered heat map

Principal component analysis (PCA) was selected as an unsupervised multivariate data analysis tool for the discrimination between the tentatively identified metabolites from the different tested extracts. The metabolites detected in ESI negative mode from *A. indica* methanol (AIW-Me), ethyl acetate (AIW-Eth.Ac.), and aqueous extract (AIW-Aq.) were plotted. Three clusters were detected in the PCA score plot (Fig. 9A). Two clusters appeared in the right upper quadrant near to each other for AIW-Me and AIW-Eth. Ac. Extracts, while the aqueous extract formed a single cluster located in the left lower quadrant. This could be attributed to the close phytochemical composition between the methanol and ethyl acetate extracts as revealed in the PCA loading plot (Fig. 9B), where they shared certain common components, *viz*., *tetra*-decyl-cyclobutanone, *oxo*-octadecadienoic

No.	Components	Class	Mol. Formula	R_t (min.)	$[M-H]^-$ *m/z*	$[M+H]^+$ *m/z*	% Composition			Ref.
							AH-Me	AH-Eth. Ac.	AH-Aq.	
1	Homovanillic acid*	Phenolic acid	$C_9H_{10}O_4$	0.21	181	–	–	–	2.87	59
2	Afzelechin	Flavonoid	$C_{15}H_{14}O_5$	0.67	273	–	–	–	6.18	61
3	3-keto-Copalic acid*	Labadane diterpenoid	$C_{20}H_{30}O_3$	0.75	317	411	(11.02)	2.87 (1.36)	–	42
4	*di*-hydro-15-Acetoxy-8,9-epoxy-labdane-19-oic acid*	Labadane diterpenoid	$C_{22}H_{34}O_5$	0.80	377	–	6.00	–	–	58
5	Umbelliferone*	Coumarin	$C_9H_6O_3$	1.11	161	–	–	–	2.44	59
6	Catechin-caffeic Acid Adduct	Cinnamic acid deriv.	$C_{24}H_{20}O_{10}$	1.42	467	–	3.14	–	2.07	98
7	Protocatechuic acid*	Phenolic acid	$C_7H_6O_4$	1.75	153	–	9.67	1.96	–	64
8	Junicedric acid*	Diterpenoid	$C_{20}H_{32}O_4$	5.42	335	–	–	–	0.23	2
9	Quercetin-pentoside	Flavonoid	$C_{20}H_{18}O_{11}$	6.33	435	524	0.85 (1.01)	–	–	99
10	Syringic acid	Phenolic acid	$C_9H_{10}O_5$	6.80	197	–	–	–	0.87	66
11	*di*-Methyl amentoflavone*	Biflavonoid	$C_{32}H_{22}O_{10}$	6.83	551	635	1.41 (0.53)	–	0.87 (1.74)	2
12	Benzoic acid derivative	Phenolic acid	–	7.01	187	–	–	–	0.45	94
13	Dodecanoic acid (Lauric acid)*	Fatty acid	$C_{12}H_{24}O_2$	7.52	199	–	–	–	0.60	59
14	*seco-iso*-Laricresinol-mono-methyl ether*	Lignan	$C_{21}H_8O_6$	8.35	375	–	–	–	1.17	2
15	Sphaeropsidin F*	Primarane diterpenoid	$C_{20}H_{32}O_4$	8.86	335	337	(5.32)	–	1.12 (0.95)	60
16	Linoleic acid	Fatty acid	$C_{18}H_{32}O_2$	9.10	279	–	0.88	1.53	1.04	96,100
17	Pimarane diterpene	Diterpenoid	$C_{20}H_{,6}$	9.60	329	–	1.73	0.64	0.46	101
18	9β,13β-Epoxy-7-abietene*	Abietane Diterpenoid	$C_{20}H_{32}O$	9.90	287	311	18.22 (6.56)	13.73 (2.70)	–	58
19	*mono*-Galloyl-hexoside	Tannin	$C_{13}H_{16}O_{10}$	10.19	331	–	1.32	–	–	54
20	Sugiol*	Abietane Diterpenoid	$C_{20}H_{28}O_2$	10.28	299	–	–	–	0.45	59
21	*tri*-Hydroxy-3,6- dimethyl-3,3α,4,5,7,7α-hexahydro-1-benzofuran-2-yl]– 3-methylbutan-1-one*	Benzofuran	$C_{15}H_{26}O_5$	10.33	285	–	–	1.55	–	68
22	Bilobetin*	Flavonoid	$C_{31}H_{20}O_{10}$	10.60	551	553	10.31 (4.78)	7.66	–	2
23	*epi*-Cupressic acid*	Labdane diterpenoid	$C_{20}H_{32}O_3$	11.49	319	–	–	–	1.05	2,58
24	*oxo*-Octadecadienoic acid	Fatty acid	$C_{18}H_{30}O_3$	11.84	293	–	–	–	0.67	94
25	(*epi*)Catechin*	Tannin	$C_{15}H_{14}O_6$	12.26	289	291	1.42 (0.55)	1.53	–	1,59
26	Acetoxy-imbricatolic acid*	Labdane diterpenoid	$C_{22}H_{36}O_4$	12.46	363	–	–	–	0.86	59
27	Ginkgetin*	Biflavonoid	$C_{32}H_{22}O_{10}$	12.58	565	567	5.15 (9.34)	7.76 (6.51)	–	1,2
28	Orientin*	Flavonoid	$C_{21}H_{20}O_{11}$	12.93	447	–	–	–	0.53	59
29	Kolavenic acid*	Clerodane diterpenoid	$C_{20}H_{32}O_2$	13.91	303	305	2.67 (1.35)	1.95	0.61	58
30	Medioresinol	Lignan	$C_{21}H_{24}O_7$	14.11	387	–	–	–	1.72	102
31	*di*-hydroxy-Octadecanoic acid*	Fatty acid	$C_{18}H_{36}O_4$	14.49	315	339	1.45 (0.77)	1.61	0.67	68
32	*tri*-methyl-Amentoflavone*	Biflavonoid	$C_{33}H_{24}O_{10}$	14.75	579	581	0.82 (7.73)	0.61 (2.31)	1.39	1,2,64
33	Syringic acid hexoside*	Phenolic acid	$C_{15}H_{20}O_{10}$	14.77	359	–	–	–	0.99	67
34	Trachylobane*	Diterpenoid	C20H32	15.00	271	–	1.79	2.55	–	2
35	hydroxy-Octadecadienoic acid	Fatty acid	$C_{18}H_{32}O_3$	15.73	295	–	1.01	–	–	51
36	Methyl-retusin	Flavonoid	$C_{17}H_{14}O_5$	16.04	297	–	0.54	0.42	1.12	63
37	Oleanolic acid	Triterpenoid	$C_{30}H_{4_8}O_3$	16.54	455	–	–	–	4.74	103
38	Acetyl-*epi*-cupressic acid*	Labdane diterpenoid	$C_{22}H_{34}O_4$	16.71	361	363	1.56 (3.14)	1.10 (1.53)	–	2,58,59
39	*tetra*-Methylamentoflavone*	Biflavonoid	$C_{34}H_{26}O_{10}$	17.07	–	595	(5.85)	(4.47)	–	1
40	*bis*-(*p*-hydroxyphenyl)-cyclopentene-one*	Norlignan	$C_{17}H_{14}O_3$	17.48	265	–	–	–	0.26	1
41	Octadecenoic acid ethyl ester*	Fatty acid	$C_{20}H_{38}O_2$	17.74	309	–	–	–	0.60	59
42	*di*-Hydroxy-octadecadienoic acid	Fatty acid	$C_{18}H_{32}O_4$	18.59	311	–	–	–	3.89	94
Continued										

No.	Components	Class	Mol. Formula	R_t (min.)	$[M-H]^-$ *m/z*	$[M+H]^+$ *m/z*	% Composition			Ref.
							AH-Me	AH-Eth. Ac.	AH-Aq.	
43	*cis*/*trans*-Cummunic acid*	Labdane diterpenoid	$C_{20}H_{30}O_2$	18.87	301	303	2.57 (1.57)	1.43	–	1,58
44	*p*-Coumaroyl-quinic acid*	Cinnamic acid deriv.	$C_{16}H_{18}O_8$	20.64	339	–	–	–	5.70	59
45	Ferruginol*	Abietane diterpenoid	$C_{20}H_{30}O$	23.29	–	287	(2.43)	(1.59)	–	59
46	Ellagic acid-pentoside*	Tannin	$C_{19}H_{14}O_{12}$	23.68	433	–	2.28	4.08	–	89
47	7-hydroxy-Labda-8(17),13(16),14-trien-19-yl-(*E*)-coumarate*	Labadane diterpenoid	$C_{30}H_{42}O_4$	24.96	459	–	–	–	1.79	59
48	*epi*-Afzelechin-hydroxybenzoate*	Flavonoid	$C_{22}H_{18}O_9$	27.47	–	395	(0.49)	–	–	59
49	Apigenin-hexoside*	Flavonoid	$C_{21}H_{20}O_{10}$	27.64	431	–	0.71	–	–	64
50	Chrysoeriol hexoside	Flavonoid	$C_{22}H_{22}O_{11}$	28.28	461	–	1.07	2.89	–	97
51	Octadecyl-ferulate (Stearyl ferulate)*	Fatty acid	$C_{28}H_{46}O_4$	28.38	445	447	(0.62)	0.99	–	1,2
52	dehydrated Lariciresinol guaiacylglyceryl ether	Lignan	–	29.37	525	–	1.39	–	–	104
53	*p*-Coumaric acid rutinoside	Cinnamic acid deriv.	$C_{15}H_{18}O_8$	30.17	471	–	2.02	–	–	47
54	Myricetin*	Flavonoid	$C_{15}H_{10}O_8$	31.16	317	–	6.03	10.46	11.31	65
55	Labda-8(17), 14-diene*	Labadane diterpene	$C_{20}H_{34}O_2$	31.34	305	307	1.57 (10.31)	1.84 (10.37)	3.04	2,58
Number of identified compounds							33	23	32	
% Identification										
ESI negative mode							87.58	69.16	61.76	
ESI positive mode							73.37	30.84	2.69	

Table 11. UPLC/MS identified metabolites from *Araucaria heterophylla* methanol, ethyl acetate and aqueous extracts. *for compounds reported before from the genus *Araucaria* and [f] for compounds reported from Family Araucariaceae. AH-Me: *Araucaria* methanol extract, AH-Eth. Ac.: *Araucaria* ethyl acetate extract, AH-Aq.: *Araucaria* aqueous extract. R_t: retention time.

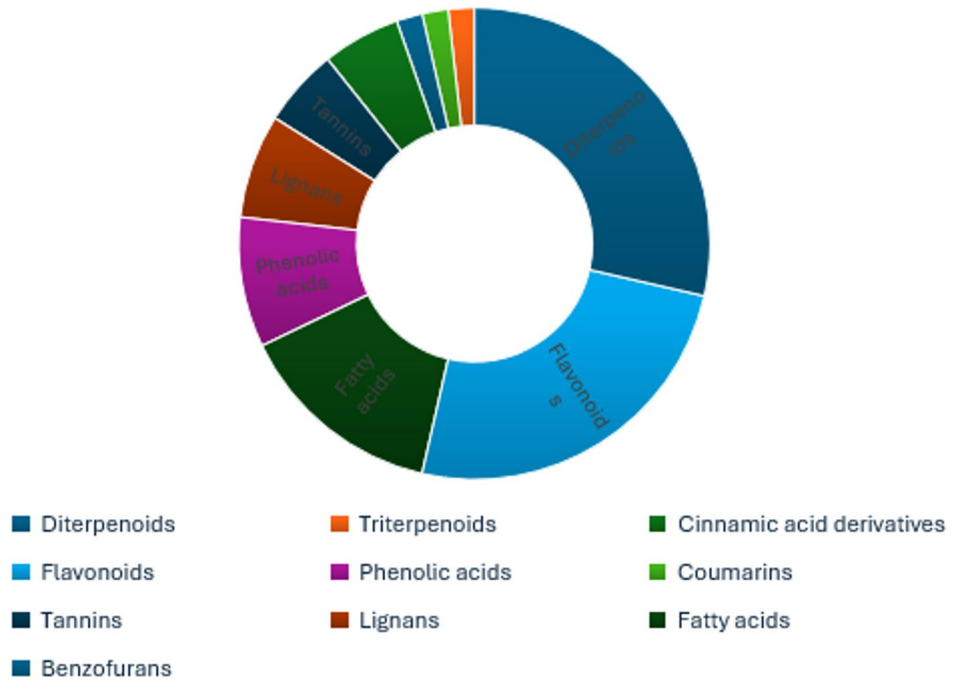

Fig. 8. A representation of the tentatively identified metabolites from *Araucaria heterophylla* extracts.

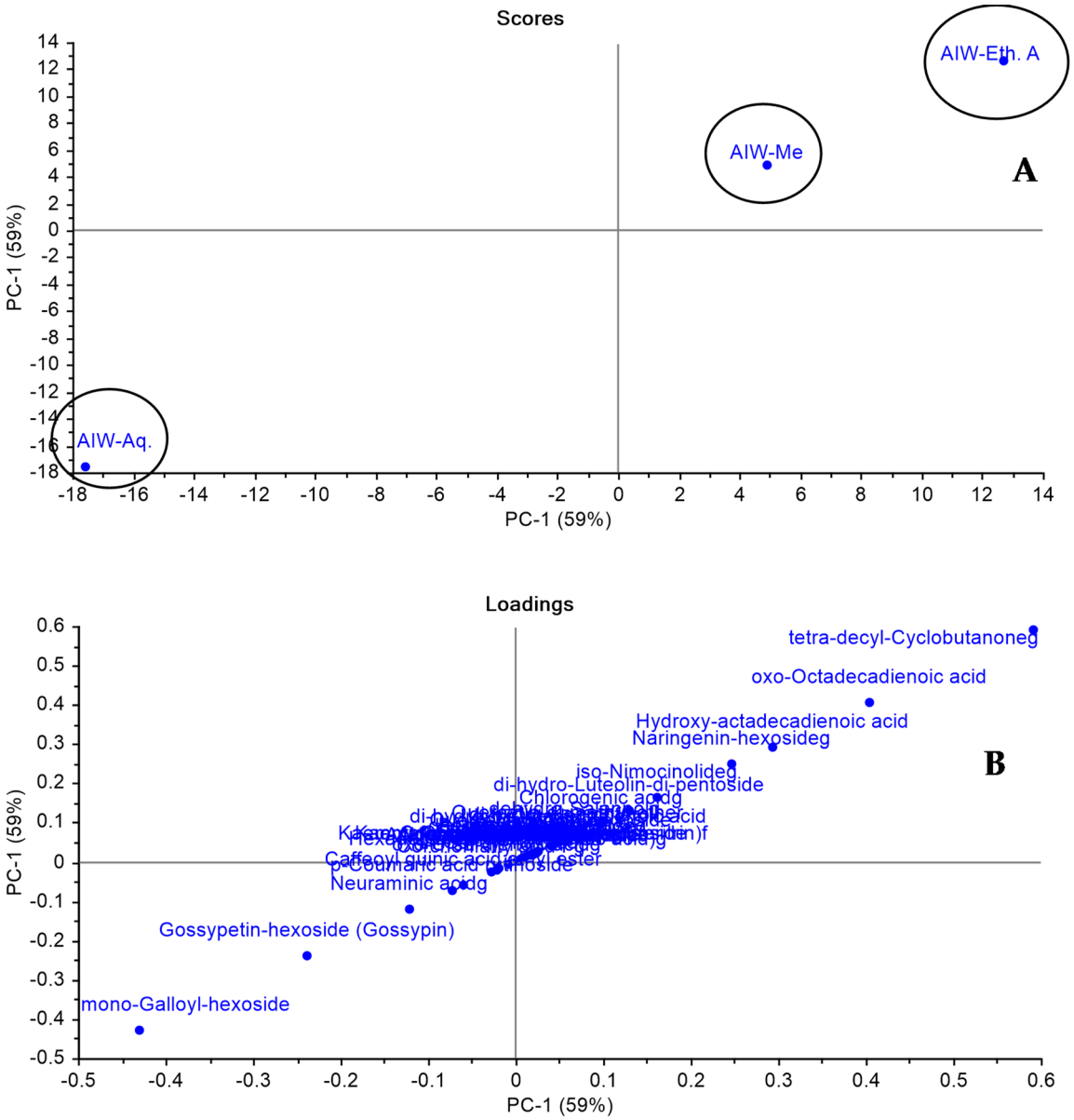

Fig. 9. (**A**) Score plot of PC1 *versus* PC2 of the UPLC/MS identified metabolites from *A. indica* methanol, ethyl acetate and aqueous extracts (area % as a variable). (**B**) Loading plot for PC1 and PC2 contributing metabolites and their assignments (area % as variable). AIW-Me: *Azadirachta indica* methanol extract, AIW-Eth. Ac.: *Azadirachta indica* ethyl acetate extract and AIW-Aq.: *Azadirachta indica* aqueous extract.

acid, hydroxyl-octodecadienoic acid, and naringenin-hexoside. While the aqueous extract showed the abundant and unique presence of gossypin and *mono*-galloyl hexoside, which explained its single clustering pattern.

Similarly, the tentatively defined metabolites from the negative ESI mode of *A. heterophylla* methanol (AH-Me), ethyl acetate (AH-Eth. Ac.) and aqueous (AH-Aq.) extracts were plotted using PCA in order to discriminate them. Three clusters were detected as illustrated in Fig. 10A, one for the AH-Aq. extract located in the left lower quadrant and two other clusters, located in the same right upper quadrant, for the AH-Me and AH-Eth. Ac. extracts. This spatial clustering pattern could be explained by the presence of unique components in abundant % composition like afzelechin and *p*-coumaroyl-quinic acid in the AH-Aq. extract. On the other hand, the other two extracts shared certain common metabolites such as 9*β*,13*β*-epoxy-7-abietene, bilobetin and protochatechuic acid which contributed to their near clusters as shown in the PCA loading plot Fig. 10B.

For further detailing and illustration, the metabolites tentatively identified in ESI negative mode from the three extracts of *A. indica* were clustered using a clustered heat map, where their previously detected clustering pattern in PCA also appeared in the clustered heat map (Fig. 11), where the color gradient ranged from green for the metabolites with the lowest % composition to red for those with the highest % composition. Likewise, the *A. heterophylla* tentatively identified metabolites in ESI negative mode were illustrated in the clustered heat map (Fig. 12), where the metabolites with the lowest % composition were in blue and those with the highest %

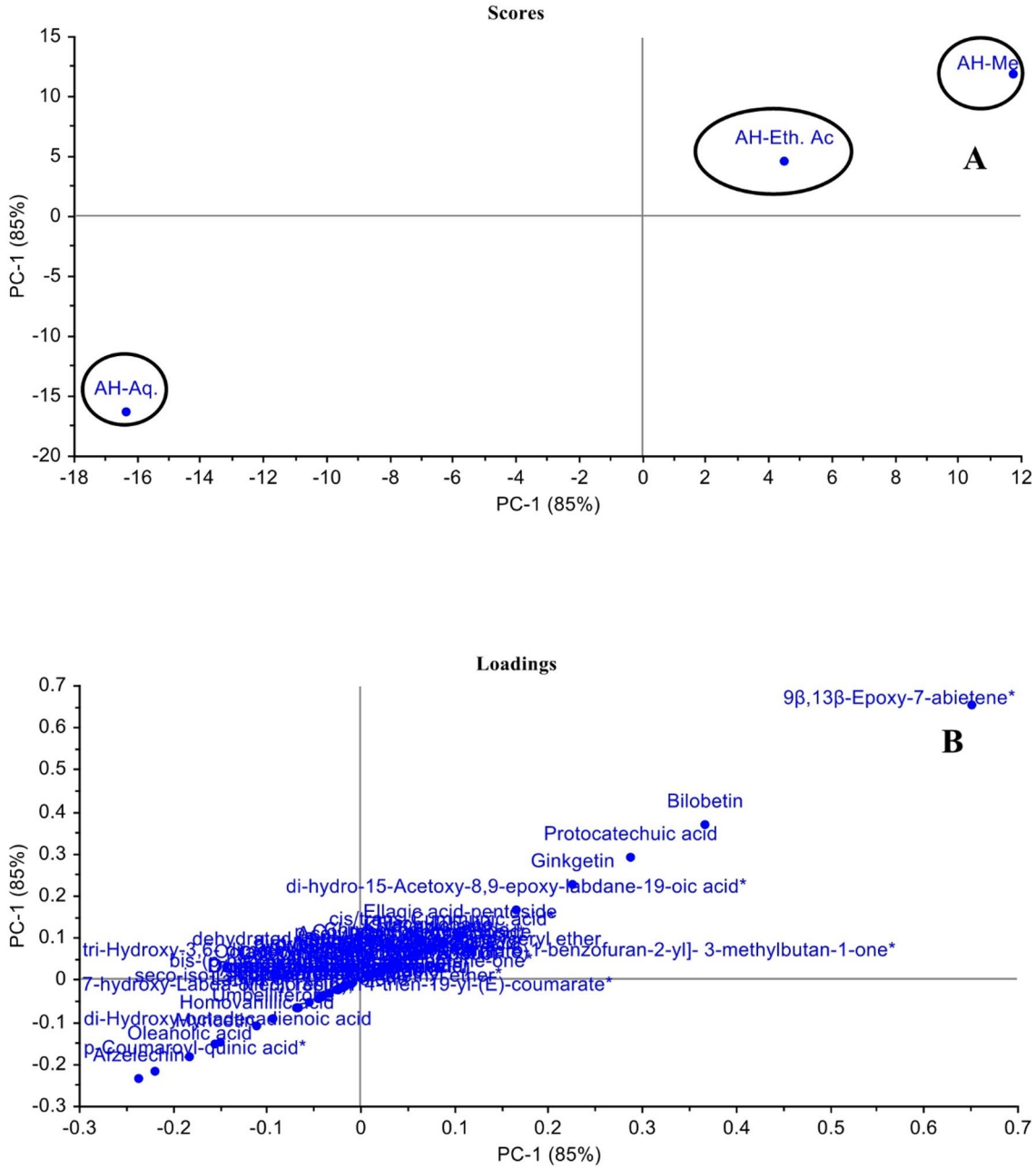

Fig. 10. (**A**) Score plot of PC1 *versus* PC2 of the UPLC/MS identified metabolites from *A. heterophylla* methanol, ethyl acetate and aqueous extracts (area % as a variable). (**B**) Loading plot for PC1 and PC2 contributing metabolites and their assignments (area % as variable). AH-Me: *Araucaria heterophylla* methanol extract, AH-Eth. Ac.: *Araucaria heterophylla* ethyl acetate extract and AH-Aq.: *Araucaria heterophylla* aqueous extract.

composition were in red. The *A. heterophylla* extracts' clustered heat map followed their same PCA clustering pattern detailed before.

Discussion

Mosquitoes remain among the most serious arthropod pests worldwide due to their role as vectors of numerous pathogens affecting human and animal health. *Culex pipiens*, in particular, is widely distributed and serves as a principal vector of West Nile virus, posing persistent epidemiological and ecological challenges. Consequently, the development of effective and environmentally compatible mosquito control strategies has become a global priority to mitigate disease transmission while minimizing ecological disruption[69].

Although chemical insecticides have long been the cornerstone of mosquito management programs, their extensive and prolonged use has led to the rapid emergence of insecticide resistance, environmental contamination, and adverse effects on non-target organisms. These limitations have intensified the search

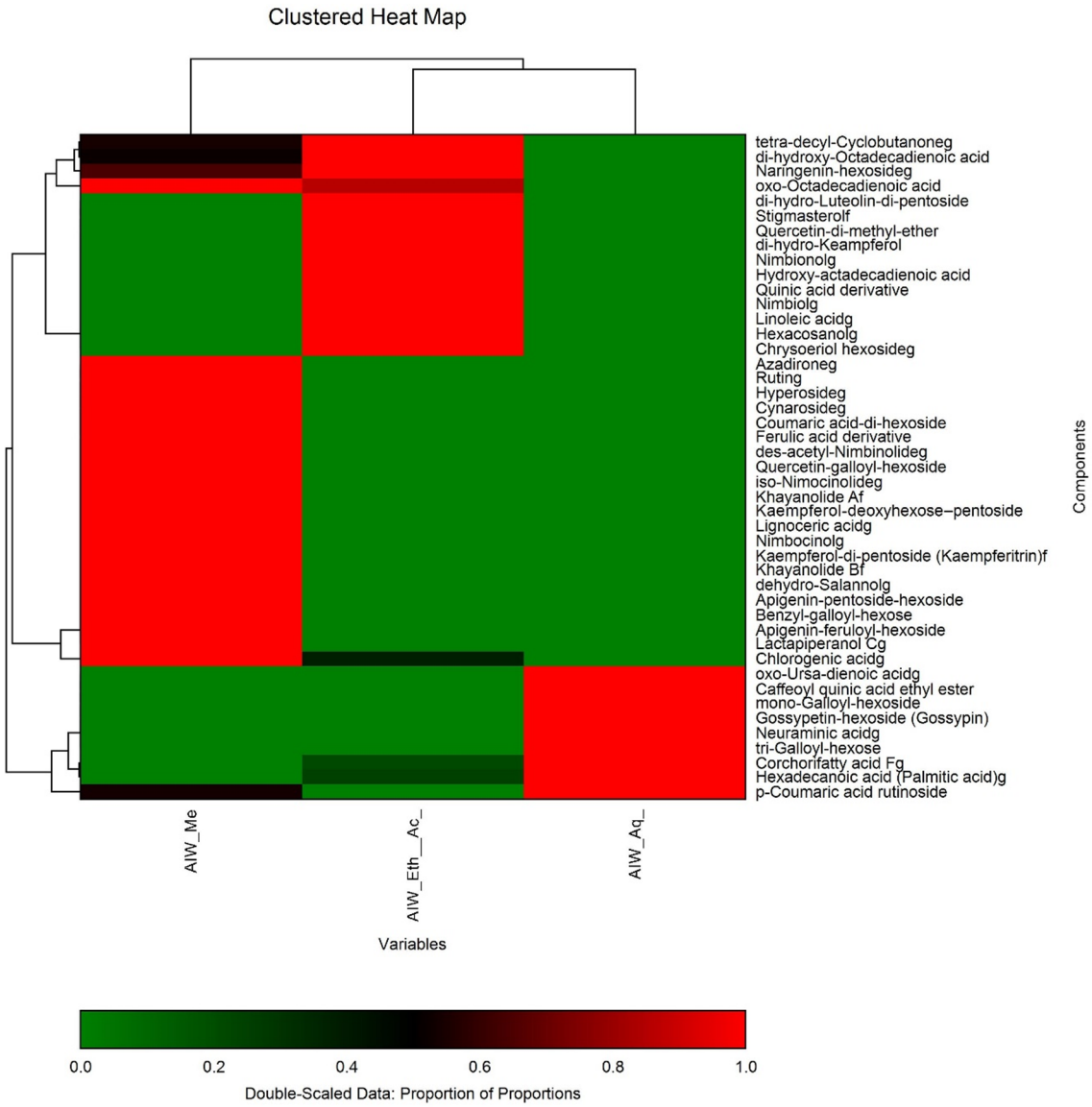

Fig. 11. Clustered heat map showing the tentatively identified metabolites (UPLC/MS, negative mode) from *A. indica* (Neem) extracts. A heat map was constructed using Euclidean distance and the unweighted group method. AIW-Me: *A. indica* methanol extract, AIW-Eth. Ac: *A. indica* ethyl acetate extract and AIW-Aq: *A. indica* aqueous extract.

for alternative, plant-based control agents that combine efficacy with ecological safety. Botanical extracts and essential oils are especially attractive due to their biodegradability, structural diversity, and multifaceted modes of action, which reduce the likelihood of resistance development[70].

Neem leaf extracts generally exhibit higher larvicidal potency than *A. heterophylla*, which may be explained by the presence of limonoids that act as potent insect growth regulators. However, both plants induce larval mortality through biochemical disruption, including inhibition of acetylcholinesterase and esterases, impairment of digestive enzymes, and induction of oxidative stress[71,72]. The suppression of antioxidant enzymes such as superoxide dismutase and catalase results in elevated levels of reactive oxygen species, causing lipid peroxidation and cellular damage in larval tissues.

Numerous investigations have demonstrated that neem leaf extracts are highly effective against *Culex pipiens*, *Aedes aegypti*, and *Anopheles* species, with larvicidal efficacy increasing in a dose- and time-dependent manner[73]. The present findings are consistent with previous reports indicating that neem extracts often outperform many other plant-based formulations due to their multifaceted modes of action, which include neurotoxicity, inhibition of digestive enzymes, and suppression of detoxification pathways[71].

Neem (*Azadirachta indica*) extracts have been shown to be effective larvicides due to their richness in bioactive compounds, particularly limonoids such as azadirachtin, as well as flavonoids, phenols, and fatty

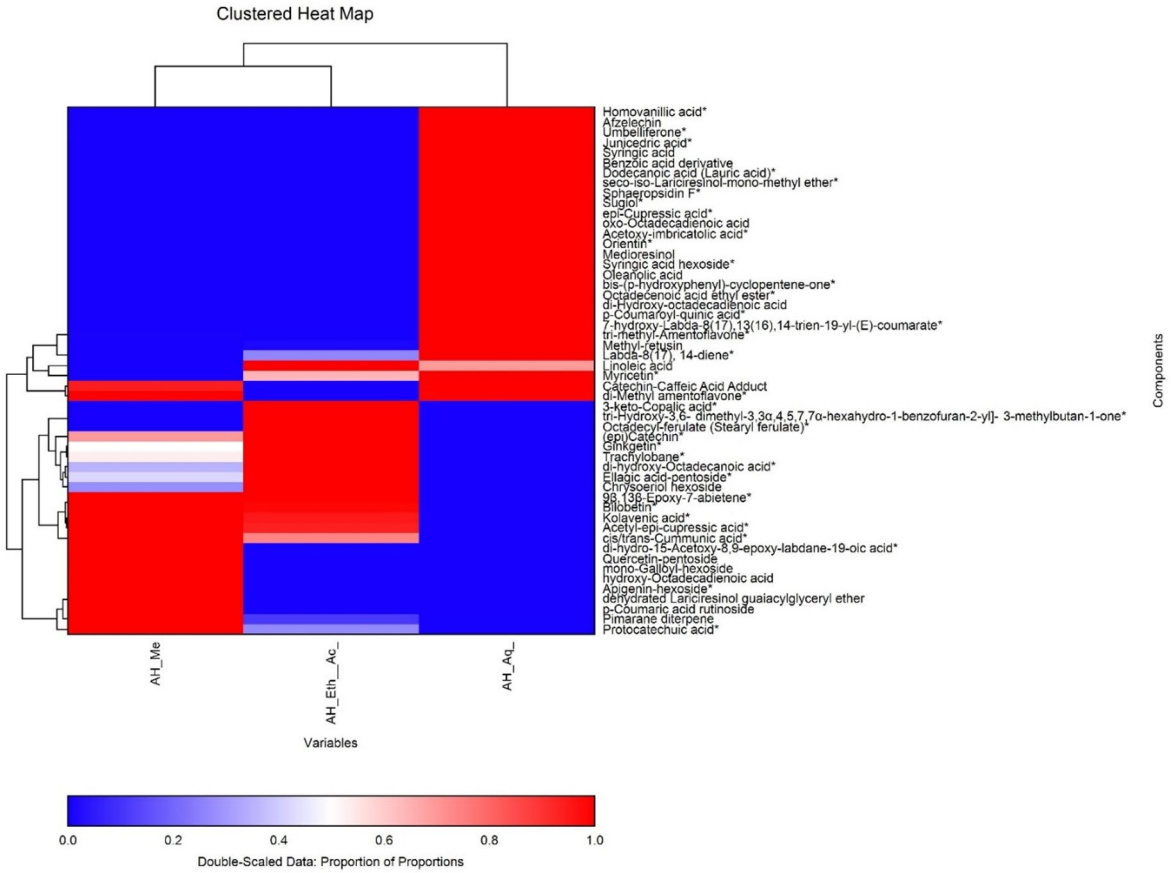

Fig. 12. Clustered heat map showing the tentatively identified metabolites (UPLC/MS, negative mode) from *A. heterophylla* extracts. A heat map was constructed using Euclidean distance and the unweighted group method. AH-Me: *A. heterophylla* methanol extract, AH-Eth. Ac: *A. heterophylla* ethyl acetate extract and AH-Aq: *A. heterophylla* aqueous extract.

acids. These compounds exert multiple toxic effects on mosquito larvae, leading to increased mortality and impaired normal development[74,75]. Among the most notable effects of neem extracts are the inhibition of larval growth and molting[76]. Azadirachtin acts as an insect growth regulator by interfering with ecdysteroid and larval hormone pathways, resulting in delayed growth, abnormal molting, and an inability to pupate[71]. These effects have been consistently reported in the larvae of *Cx. pipiens*, *Aedes aegypti*, and *Anopheles* mosquitoes, with treated larvae exhibiting prolonged larval stages and morphological deformities before death[73,77,78].

Neem extracts also exhibit direct neurotoxic effects by inhibiting acetylcholinesterase (AChE) activity, leading to an accumulation of acetylcholine at synapses and subsequent neurological dysfunction, paralysis, and death[79]. Furthermore, neem-derived compounds inhibit detoxification enzymes such as esterases, reducing the larvae's ability to metabolize toxins.

Studies have shown that neem extracts inhibit the action of key digestive enzymes, including amylase, lipase, and protease, reducing nutrient absorption and energy availability, ultimately leading to poor larval survival[71,80]. Neem's potent anti-nutritional properties further exacerbate energy depletion and growth failure. Moreover, neem treatment of larvae induces oxidative stress, characterized by decreased activity of antioxidant enzymes such as superoxide dismutase (SOD), catalase (CAT), and glutathione S-transferase (GST), accompanied by increased lipid peroxidation and protein oxidation[81]. This oxidative imbalance leads to cell damage and significantly contributes to larval mortality.

Due to their multiple and synergistic mechanisms of action, neem extracts are less likely to induce resistance development compared to conventional synthetic insecticides. Furthermore, their biodegradability and low relative toxicity to non-target organisms make neem formulations promising candidates for environmentally sustainable mosquito larvae control within integrated vector management programs[82].

The enhanced efficacy of nanoemulsions can be attributed to their small droplet size, improved dispersion, and increased surface area, which facilitate greater penetration through the larval cuticle and more efficient delivery of active compounds to target tissues. These findings align with previous studies demonstrating that nanoemulsion-based botanical formulations outperform conventional extracts due to improved stability, controlled release, and prolonged bioactivity. The superior performance of *A. indica* formulations is consistent

with its well-documented insecticidal reputation, largely attributed to limonoids, flavonoids, and phenolic compounds known to disrupt insect growth, feeding behavior, and neurophysiological processes[83].

Phytochemical profiling using GC/MS and UPLC/MS revealed a rich and diverse array of metabolites in both plants, supporting their larvicidal activity. The *A. heterophylla* extracts were characterized by a high abundance of diterpenoids, sesquiterpenoids, flavonoids, fatty acids, and phenolic acids, compounds previously reported to exert toxic, repellent, and growth-inhibitory effects on insects[12]. In contrast, *A. indica* extracts were particularly enriched in flavonoids, limonoids, cinnamic acid derivatives, and fatty acids, many of which are recognized for their potent insecticidal and antifeedant properties[84]. The diversity and complexity of these phytochemicals likely contribute to synergistic interactions that enhance overall toxicity and reduce the risk of resistance development.

Biochemical analyses further elucidated the mode of action underlying the observed larvicidal effects. Exposure of *Cx. pipiens* larvae to LC_{50} concentrations of both plant extracts and their nanoemulsions resulted in pronounced inhibition of detoxification enzymes, metabolic enzymes, and antioxidant defense systems. The suppression of esterases and acetylcholinesterase suggests interference with neural transmission and detoxification pathways, leading to impaired physiological function and eventual mortality. Additionally, the inhibition of metabolic enzymes such as amylase and lipase indicate disruption of energy metabolism, further weakening larval viability.

The marked reduction in antioxidant enzymes (SOD, GST, CAT, and GSH), accompanied by increased lipid peroxidation and protein carbonylation, demonstrates that oxidative stress plays a central role in larval toxicity. The stronger biochemical disturbances observed in larvae treated with *A. indica* nanoemulsion corroborate its higher larvicidal efficacy and highlight its capacity to overwhelm larval defense mechanisms. These results are consistent with earlier reports indicating that plant-derived compounds can induce oxidative imbalance, cellular damage, and apoptosis-like effects in mosquito larvae.

The effectiveness of the nanoemulsion formulations was further supported by comprehensive physicochemical characterization. UV–visible spectroscopy confirmed successful encapsulation of bioactive compounds, while dynamic light scattering and zeta potential analyses indicated stable colloidal systems with acceptable size distribution and electrostatic stability. Transmission electron microscopy provided direct evidence of nanoscale, spherical droplets, confirming that both *A. heterophylla* and *A. indica* extracts were successfully converted into stable nanoemulsions suitable for biological application. The discrepancy between hydrodynamic size (DLS) and core size (TEM) is expected and reflects the presence of a hydration layer and surface-bound metabolites, a characteristic feature of well-formed nanoemulsions.

From an applied perspective, the findings of this study reinforce the potential of plant-based nanoformulations as effective and sustainable alternatives to synthetic insecticides. The complex mixture of phytochemicals presents in *A. heterophylla* and *A. indica* extracts provides multiple modes of action, reducing the probability of resistance development and enhancing compatibility with integrated vector management programs. Moreover, nanoemulsion technology addresses key limitations of botanical insecticides, such as volatility and short residual activity, by improving stability, persistence, and bioavailability.

The current study involved a comparative phytochemical profiling for different extracts of *Azadirachta indica* and *Araucaria heterophylla*. The profiling involved the GC/MS analysis for the n-hexane extracts as well as the UPLC/MS analysis of the methanol, ethyl acetate, and aqueous extracts of the two plants. The GC/MS analysis for the n-hexane extracts revealed the presence of common phytochemical classes like long-chain alkanes and alkyl-substituted benzene derivatives between the two plants. However, marked qualitative differences were observed between the two n-hexane extracts. The *A. heterophylla* n-hexane extract showed a notable terpenoid composition exemplified as sesquiterpenoids and oxygenated terpenoids such as caryophyllene, humulene, β-bisabolene, carotol, and kaurene derivatives, which are usually linked to plant defense and ecological interactions. On the other hand, *A. indica* n-hexane extract showed an abundant profile of fatty acids and their derivatives, viz., methyl esters of palmitic and stearic acids, along with long-chain branched alkanes and alcohols.

Likewise, the UPLC/MS profiling of each plant's extracts revealed that both neem and Christmas tree extracts carried common components such as oleanolic acid, chrysoeriol hexoside, mono-galloyl hexoside, *p*-coumaric acid-rutinoside, and different fatty acids, including linoleic acid and oxo- and hydroxy-octadecadienoic acid derivatives, which indicated a certain level of similarity between the two plants. However, each group of extracts for each plant involved a unique and characteristic phytochemical profile probably linked to its biological effects. The neem extracts presented a pronounced and abundant presence of limonoids and related triterpenoids, particularly azadirachtin-type and khayanolide derivatives, suggesting a metabolic specialization toward highly oxygenated tetranortriterpenes typically linked to chemodefensive functions. In addition to galloylated flavonoids and phenolic acids. Conversely, the second profile is characterized by an extensive array of diterpenoids belonging to labdane, abietane, pimarane, clerodane, and trachylobane skeletons, alongside biflavonoids, lignans, phenolic acids, and benzofuran derivatives, indicating a distinct diterpene- and phenylpropanoid-oriented metabolism.

The observed phytochemical profile for the two plants in the current study matched their documented literature records. For instance, *A. indica* leaf extract was profiled using ICP-MS, and it was rich with phenolic acids, including tannic and salicylic acid, with major flavonoids being hyperoside, kaempferol, and quercetin. In addition to certain water-soluble vitamins like nicotinic acid, nicotinamide, and pantothenic acid, followed by pyridoxine, thiamine, and riboflavin. The ethanol extract exhibited moderate antioxidant activity (30.02% inhibition of ABTS radicals; IC50 0.918 µg/mL for CUPRAC) and low inhibition of BChE and AChE (2.29% and 3.17%, respectively)[35].

In another study, the ethanol fruit extract of *A. indica* contained desacetylnimbinolide, nimbidiol, *O*-methylazadironolide, nimbidic acid, and desfurano-6α-hydroxyazadiradione, as revealed by LC/MS analysis. The ethanol extract resulted in 83% suppression at 800 mg/kg, while 84% parasitemia clearance was obtained in the curative study against malaria[8]. Likewise, the aqueous leaf extract of *A. indica* was reported to contain

quercetin and cynaroside as well as aurachin D, gentisic acid, allivicin, lactapiperanol C, bruceantin, and caulerpin, and copalliferol B through HPLC-MS analysis[30].

Regarding the genus *Araucaria*, two biflavonoids were isolated from the acetone extracts of *A. hunsteinii* twigs and *A. columnaris* leaves. The identified compounds were 4',4''',7,7''-*tetra*-*O*-methylcupressuflavone and 7-*O*-methylcupressuflavone[59]. In another study, *A. araucana* phytochemical composition revealed the presence of three lignans, namely, eudesmin, ((1 S,2R,3R)-1,2,3,4-tetrahydronaphthalene-2,3-diyl) dimethanol, and secoisolariresinol[85].

The acetone extract of *A. columnaris* showed the presence of 4',4''',7,7''-*tetra*-*O*-methylcupressuflavone, which exhibited IC50 values of 272.95 ± 7.05 and 239.36 ± 13.50 μg/mL, respectively, against CPAE cells. In addition, 4',7,7''-*tri*-*O*-methylcupressuflavone and 4''',7-*di*-*O*-methylcupressuflavone showed high activity with IC_{50} values of 39.5 ± 1.44 and 66.13 ± 15.96 μg/mL, respectively. Although none of the individual components demonstrated any detectable antioxidant activity (IC_{50} > 100 μg/mL), the acetone extract showed moderate antioxidant activity with an IC_{50} value of 69.2 μg/mL [86].

Conclusions

The present study demonstrates that nanoemulsions of *Araucaria heterophylla* and *Azadirachta indica* significantly enhance larvicidal efficacy against *Culex pipiens* through combined physicochemical optimization, biochemical disruption, and oxidative stress induction. These findings support the incorporation of plant-based nanoemulsions into environmentally sustainable mosquito control strategies and highlight their promise as safer alternatives to conventional chemical insecticides. Comprehensive GC/MS and UPLC/MS profiling revealed marked phytochemical diversity between *Araucaria heterophylla* and *Azadirachta indica* across different solvent extracts. A characteristic and distinct phytochemical profile was observed, with *Araucaria heterophylla* extracts mainly characterized by a diterpenoid- and sesquiterpenoid-rich profile, while *Azadirachta indica* extracts were dominated by flavonoids, limonoids, and fatty acid derivatives. These findings highlight the influence of plant species and extraction polarity on metabolite composition and support the potential of both plants as valuable sources of bioactive natural products. These findings support the potential application of these plant-based formulations as eco-friendly, sustainable alternatives for mosquito control, while further in vivo and clinical studies could elucidate their safety and optimize their use in vector management programs.

Data availability

The datasets used and/or analyzed during the current study available from the corresponding author on reasonable request. Correspondence: [mohamed.albaz@fsc.bu.edu.eg](mailto: mohamed.albaz@fsc.bu.edu.eg).

Received: 18 January 2026; Accepted: 31 March 2026
Published online: 06 May 2026

References

1. Peralta, R. M. et al. Biological activities and chemical constituents of *Araucaria angustifolia*: An effort to recover a species threatened by extinction. *Trends Food Sci. Technol.* **54**, 85–93 (2016).
2. Aslam, M. S., Choudhary, B. A., Uzair, M. & Ijaz, A. S. Phytochemical and ethno-pharmacological review of the genus *Araucaria*–review. *Trop. J. Pharm. Res.* **12**, 651–659 (2013).
3. Elshamy, A. I. et al. Essential oil and its nanoemulsion of *Araucaria heterophylla* resin: Chemical characterization, anti-inflammatory, and antipyretic activities. *Ind. Crops Prod.* **148**, 112272 (2020).
4. Abd Elmohsen, M., Selim, A. & Abd Elmoneim, A. E. Prevalence and molecular characterization of Lumpy Skin Disease in cattle during period 2016–2017. *Benha Veterinary Med. J.* **37**, 172–175 (2019).
5. Hamdy, A. S., Selim, A., Shoulah, S. A. & Ibrahim, A. M. M. Sero-surveillance infectious bovine rhinotracheitis in ruminants and assessment the associated risk factors. *Benha Veterinary Med. J.* **42**, 160–163 (2022).
6. Jaramillo, D. et al. Chemical characterization and biological activity of the essential oil from *Araucaria brasiliensis* collected in Ecuador. *Molecules* **27**, 3793 (2022).
7. Hol, F. J., Lambrechts, L. & Prakash, M. BiteOscope, an open platform to study mosquito biting behavior. *Elife* **9**, e56829 (2020).
8. Faloye, K. O. et al. LC-MS analysis, computational investigation, and antimalarial studies of *Azadirachta indica* fruit. *Bioinform. Biol. insights*. **17**, 11779322231154966 (2023).
9. Jessinta, A. Chemical Characterization and Biological Studies of Neem *(Azadirachta indica)* Extracts (University Malaysia Pahang, 2014).
10. Martínez-Romero, A., Ortega-Sánchez, J. L., Hernández-González, S. I., Olivas-Calderón, E. H. & Alba-Romero, J. J. Application of neem tree in agriculture, industry, medicine, and environment: A review. *Afr. J. Tradit. Complement. Altern. Med.* **13**, 191–198 (2016).
11. Debnath, S., Das, M., Mondal, S., Sarkar, B. K. & Babu, G. Neem (*Azadirachta indica* A. Juss): a multifaceted tree & an elixir in the traditional system of Indian medicine. *Discover Plants*. **2**, 156 (2025).
12. Baz, M. M., Selim, A., Radwan, I. T., Alkhaibari, A. M. & Khater, H. F. Larvicidal and adulticidal effects of some Egyptian oils against *Culex pipiens*. *Sci. Rep.* **12**, 4406 (2022).
13. Madhav, M., Blasdell, K. R., Trewin, B., Paradkar, P. N. & López-Denman, A. J. *Culex*-transmitted diseases: mechanisms, impact, and future control strategies using Wolbachia. *Viruses* **16**, 1134 (2024).
14. Baz, M. M. et al. Efficiency of *Datura stramonium* metabolites as a promising insecticide against the vector-borne diseases *Culex pipiens* and *Aedes aegypti*. *Parasitology International*, 103178 (2025).
15. Radwan, I. T., Baz, M. M., Khater, H. & Selim, A. M. Nanostructured lipid carriers (NLC) for biologically active green tea and fennel natural oils delivery: Larvicidal and adulticidal activities against *Culex pipiens*. *Molecules* 27, (2022). (1939).
16. WHO. *Guidelines for laboratory and field testing of mosquito larvicides* (World Health Organization, 2005).
17. Ellman, G. L., Courtney, K. D., Andres Jr, V. & Featherstone, R. M. A new and rapid colorimetric determination of acetylcholinesterase activity. *Biochem. Pharmacol.* **7**, 88–95 (1961).
18. Penilla, P. R. et al. Resistance management strategies in malaria vector mosquito control. Baseline data for a large-scale field trial against *Anopheles albimanus* in Mexico. *Med. Vet. Entomol.* **12**, 217–233 (1998).
19. Bradford, M. M. A rapid and sensitive method for the quantitation of microgram quantities of protein utilizing the principle of protein-dye binding. *Anal. Biochem.* **72**, 248–254 (1976).

20. Boer, T. D. & Bruinvels, J. Assay and properties of 4-aminobutyric-2-oxoglutaric acid transaminase and succinic semialdehyde dehydrogenase in rat brain tissue. *J. Neurochem.* **28**, 471–478 (1977).
21. Ishaaya, I. & Swirski, E. Invertase and amylase activity in the armoured scales *Chrysomphalus aonidum* and Aonidiella aurantii. *J. Insect. Physiol.* **16**, 1599–1606 (1970).
22. Itaya, K. A more sensitive and stable colorimetric determination of free fatty acids in blood. *J. Lipid Res.* **18**, 663–665 (1977).
23. Nishikimi, M., Rao, N. A. & Yagi, K. The occurrence of superoxide anion in the reaction of reduced phenazine methosulfate and molecular oxygen. *Biochem. Biophys. Res. Commun.* **46**, 849–854 (1972).
24. Habig, W. H., Pabst, M. J. & Jakoby, W. B. Glutathione S-transferases: the first enzymatic step in mercapturic acid formation. *J. Biol. Chem.* **249**, 7130–7139 (1974).
25. Beutler, E., Duron, O. & Kelly, B. M. Improved method for determination of blood glutathione. (1963).
26. Ohkawa, H., Ohishi, N. & Yagi, K. Assay for lipid peroxides in animal tissues by thiobarbituric acid reaction. *Anal. Biochem.* **95**, 351–358 (1979).
27. Levine, R. L., Williams, J. A., Stadtman, E. P. & Shacter, E. in *Methods enzymology* **233** 346–357 (Elsevier, 1994).
28. Islam, M. N., Downey, F. & Ng, C. Comprehensive profiling of flavonoids in *Scutellaria incana* L. using LC-Q-TOF-MS. *Acta Chromatogr.* **25**, 555–569 (2013).
29. Hassan, W. H., Abdelaziz, S. & Al Yousef, H. M. Chemical composition and biological activities of the aqueous fraction of *Parkinsonea aculeata* L. growing in Saudi Arabia. *Arab. J. Chem.* **12**, 377–387 (2019).
30. Bokkar, S. et al. High resolution liquid chromatography-mass spectrometry analysis (Q-TOF-MS) and free radical scavenging activity of extract of *Azadirachta indica* leaves. *Haryana Vet.* **62**(2): 122–128.
31. Salih, E. Y. et al. LC-MS/MS tandem mass spectrometry for analysis of phenolic compounds and pentacyclic triterpenes in antifungal extracts of *Terminalia brownii* (Fresen). *Antibiotics* **6**, 37 (2017).
32. Sun, Y. et al. Profiling of volatile and non-volatile compounds in Dianhong by a combined approach of static headspace GC-MS and UPLC-MS. *CyTA-Journal Food*. **20**, 305–315 (2022).
33. Beelders, T., De Beer, D., Stander, M. A. & Joubert, E. Comprehensive phenolic profiling of *Cyclopia genistoides* (L.) Vent. by LC-DAD-MS and-MS/MS reveals novel xanthone and benzophenone constituents. *Molecules* **19**, 11760–11790 (2014).
34. Singh, N. & Singh, P. P. Structure-Based Virtual Screening of Phytochemicals from *Phyllanthus amarus* as Potent Inhibitory Phytocompounds Against Marburg Virus Disease. *Receptor* 8, 9 (2023).
35. Boukeloua, A. et al. A comprehensive study on chemical and biological profiles of Algerian *Azadirachta indica* (A. Juss). *Phytochem. Lett.* **61**, 89–96 (2024).
36. Hamdan, D. I. et al. *Salix subserrata* bark extract-loaded chitosan nanoparticles attenuate neurotoxicity induced by sodium arsenate in rats in relation with HPLC–PDA-ESI–MS/MS profile. *AAPS PharmSciTech*. **24**, 15 (2022).
37. Huma, Z. et al. *Azadirachta indica*-based green fabrication of metal oxide nanoparticles: a state-of-the-art review. *Nano Biomed. Engineering* (2024).
38. El-Nashar, H. A. et al. UPLC-ESI/MSn metabolic profiling of *Cedrela odorata* L. and *Toona ciliata* M. Roem and in vitro investigation of their anti-diabetic activity supported with molecular docking studies. *Front. Chem.* **12**, 1462309 (2024).
39. Elhawary, E. A. et al. Sustainable MnO_2/MgO bimetallic nanoparticles capped with sword fern methanol extract attain Antioxidant/Anti-Biofilm potential: A UPLC-ESI/LC/MS and network Pharmacology-Supported study. *Pharmaceuticals* **18**, 1262 (2025).
40. Zuleta-Castro, C. et al. In vitro antiplasmodial activity of an *Azadirachta indica* cell culture extract. *Proceedings of the National Academy of Sciences, India Section B: Biological Sciences* 91, 81–88 (2021).
41. Ji, K. L. et al. Limonoids from the fruits of *Khaya ivorensis*. *Molecules* **19**, 3004–3011 (2014).
42. Santos, K. S. et al. Antiproliferative activity of neem leaf extracts obtained by a sequential pressurized liquid extraction. *Pharmaceuticals* **11**, 76 (2018).
43. Thavamani, L. et al. Phytochemical Analysis (LC-MS) of *Azadirachta Indica* Ethanolic Extract, Antioxidant, Anticancer, in Vitro Wound Healing Activity, and Immunomodulatory Effects of *Azadirachta indica* Ethanolic Extract. *Journal Adv. Zoology* **44** (2023).
44. Marin-Saez, J., López-Ruiz, R., Romero-Gonzalez, R. & Garrido Frenich, A. Comprehensive dissipation of azadirachtin in grapes and tomatoes: The effect of *Bacillus thuringiensis* and tentative identification of unknown metabolites. *J. Agric. Food Chem.* **71**, 4466–4476 (2023).
45. Liu, C. et al. Chemical profiling of kaliziri injection and quantification of six caffeoyl quinic acids in beagle plasma by LC-MS/MS. *Pharmaceuticals* **15**, 663 (2022).
46. Marzouk, M. M. et al. C-glycosyl flavonoids-rich extract of *Dipcadi erythraeum* Webb & Berthel. bulbs: Phytochemical and anticancer evaluations. *J. Appl. Pharm. Sci.* **9**, 094–098 (2019).
47. Elgendi, S., Ezzat, M., Elsayed, A. & HPLC-PDA-ESI-MS -MS analysis of acids content of *Lantana camara* L. flower extract and its anticoagulant activity. *Egypt. J. Chem.* **66**, 249–256 (2023).
48. Bystrom, L. M., Lewis, B. A., Brown, D. L., Rodriguez, E. & Obendorf, R. L. Characterisation of phenolics by LC–UV/Vis, LC–MS/MS and sugars by GC in *Melicoccus bijugatus* Jacq.'Montgomery'fruits. *Food Chem.* **111**, 1017–1024 (2008).
49. Schütz, K., Kammerer, D. R., Carle, R. & Schieber, A. Characterization of phenolic acids and flavonoids in dandelion (*Taraxacum officinale* WEB. ex WIGG.) root and herb by high-performance liquid chromatography/electrospray ionization mass spectrometry. *Rapid Commun. Mass. Spectrometry: Int. J. Devoted Rapid Dissemination Up-to-the-Minute Res. Mass. Spectrom.* **19**, 179–186 (2005).
50. AĞALAR, H., Ciftci, G., Göger, F. & KIRIMER, N. Activity guided fractionation of *Arum italicum* miller tubers and the LC/MS-MS profiles. *Records Nat. Products* **12** (2018).
51. Grati, W. et al. HESI-MS/MS analysis of phenolic compounds from *Calendula aegyptiaca* fruits extracts and evaluation of their antioxidant activities. *Molecules* **27**, 2314 (2022).
52. Baz, M. M. et al. Efficacy of Hot *Capsicum annuum* Extracts Against the Biological Activity of *Culex pipiens* and *Musca domestica* Larvae with their Phytochemical Profiles. *Acta Parasitol.* **70**, 129 (2025).
53. Elhawary, E. A. et al. Seasonal variation effect on different *Physalis peruviana* L.(Solanaceae) waste extracts and investigation of their efficacy against *Culex pipiens* and *Musca domestica*. *Sci. Rep.* **15**, 20231 (2025).
54. Raslan, M., Abdel Rahman, R., Fayed, H., Ogaly, H. & Fikry, R. Metabolomic profiling of *Sansevieria trifasciata* hort ex. Prain leaves and roots by HPLC-PAD-ESI/MS and its hepatoprotective effect *via* activation of the NRF_2/ARE signaling pathway in an experimentally induced liver fibrosis rat model. *Egypt. J. Chem.* **64**, 6647–6671 (2021).
55. Kashchenko, N. I., Olennikov, D. N. & Chirikova, N. K. Metabolites of *Siberian raspberries*: LC-MS profile, seasonal variation, antioxidant activity and, thermal stability of *Rubus matsumuranus* phenolome. *Plants* **10**, 2317 (2021).
56. Li, C. & Seeram, N. P. Ultra-fast liquid chromatography coupled with electrospray ionization time-of-flight mass spectrometry for the rapid phenolic profiling of red maple (*Acer rubrum*) leaves. *J. Sep. Sci.* **41**, 2331–2346 (2018).
57. El-Shazly, M. A., Hamed, A. A., Kabary, H. A. & Ghareeb, M. A. LC-MS/MS profiling, antibiofilm, antimicrobial and bacterial growth kinetic studies of *Pluchea dioscoridis* extracts. *Acta Chromatographica* (2021).
58. Sweilam, S. H. et al. A first metabolite analysis of Norfolk Island pine resin and its hepatoprotective potential to alleviate methotrexate (MTX)-induced hepatic injury. *Pharmaceuticals* **17**, 970 (2024).
59. Frezza, C. et al. Phytochemistry, chemotaxonomy, and biological activities of the Araucariaceae family—A review. *Plants* **9**, 888 (2020).

60. Hanson, J. R., Nichols, T., Mukhrish, Y. & Bagley, M. C. Diterpenoids of terrestrial origin. *Nat. Prod. Rep.* **36**, 1499–1512 (2019).
61. Ben Said, R. et al. Tentative characterization of polyphenolic compounds in the male flowers of *Phoenix dactylifera* by liquid chromatography coupled with mass spectrometry and DFT. *Int. J. Mol. Sci.* **18**, 512 (2017).
62. Stănilă, A. et al. Extraction and characterization of phenolic compounds from rose hip (*Rosa canina* L.) using liquid chromatography coupled with electrospray ionization-mass spectrometry. *Notul. Botan. Horti Agrobotan.Cluj-Napoca*. **43**, 349–354 (2015).
63. Ye, M. et al. Characterization of flavonoids in *Millettia nitida* var. *hirsutissima* by HPLC/DAD/ESI-MS^n. *J. Pharm. Anal.* **2**, 35–42 (2012).
64. El-Hawary, S. S. et al. Metabolomic profiling of three *Araucaria* species, and their possible potential role against COVID-19. *J. Biomol. Struct. Dynamics*. **40**, 6426–6438 (2022).
65. Sugita, P. et al. The cytotoxicity and SAR analysis of biflavonoids isolated from *Araucaria hunsteinii* K. Schum. leaves against MCF-7 and HeLa cancer cells. *J. Appl. Pharm. Sci.* **13**, 199–209 (2023).
66. Slimen, I. B., Mabrouk, M., Hanène, C., Najar, T. & Abderrabba, M. LC-MS analysis of phenolic acids, flavonoids and betanin from spineless *Opuntia ficus-indica* fruits. *Cell. Biol.* **5**, 17–28 (2017).
67. Younis, N., Zafer, M. & Elosaily, A. Phytochemical characterization, antioxidant potential and antibacterial activity of *Araucaria columnaris* against methicillin-resistant *Staphylococcus aureus* (MRSA) and *Streptococcus pyogenes*. *J. Adv. Pharm. Res.* **8**, 121–134 (2024).
68. Ye, L. et al. LC-MS/MS-based metabolomic of pink *Auricularia cornea* grown on *Lycium barbarum* sawdust substrate. *Food Chem.* **482**, 144198 (2025).
69. Baz, M. M. et al. Chemical composition and bio-efficacy of agro-waste plant extracts and their potential as bioinsecticides against *Culex pipiens* mosquitoes. *Parasitol. Int.* **104**, 102968 (2025).
70. Barik, T. K. et al. Impact of insecticide resistance on controlling mosquito vectors and its potential contribution to behavioural modifications. *Malaria Journal* (2025).
71. Senthil-Nathan, S. Physiological and biochemical effect of neem and other Meliaceae plants secondary metabolites against Lepidopteran insects. *Front. Physiol.* **4**, 359 (2013).
72. Hikal, W. M. & Said-Al Ahl, H. A. Influence of *Plectranthus amboinicus* essential oil on potentially pathogenic Acanthamoeba isolated from water tanks in Tabuk, Saudi Arabia. *Env Cons*. **25**, 1137–1145 (2019).
73. Govindarajan, M., Rajeswary, M. & Benelli, G. Chemical composition, toxicity and non-target effects of *Pinus kesiya* essential oil: An eco-friendly and novel larvicide against malaria, dengue and lymphatic filariasis mosquito vectors. *Ecotoxicol. Environ. Saf.* **129**, 85–90 (2016).
74. Nisbet, A. J. Azadirachtin from the neem tree *Azadirachta indica*: its action against insects. *Anais da Sociedade Entomológica do Brasil*. **29**, 615–632 (2000).
75. Chatterjee, S. et al. Neem-based products as potential eco-friendly mosquito control agents over conventional eco-toxic chemical pesticides-A review. *Acta Trop.* **240**, 106858 (2023).
76. Rashid, M. & Ahmad, A. The effect of neem (*Azadirachta indica*) leaves extract on the ecdysis and mortality of immature stages of common house mosquito *Culex pipiens* fatigans. *Biol. (Pakistan)*. **59**, 213–219 (2013).
77. Awosolu, O., Adesina, F. & Iweagu, M. Larvicidal effects of croton (*Codiaeum variegatum*) and Neem (*Azadirachta indica*) aqueous extract against *Culex* mosquito. (2018).
78. Aziz, A. T. A comparative study and characterization of *Azadirachta indica* mediated nano-insecticide and ethanolic extract against mosquito vectors–Arabian and Indian strains. *Entomol. Res.* **51**, 559–567 (2021).
79. Fakunle, P. et al. Assessment of the Ameliorative Effects of Aqueous Neem (*Azadirachta Indica*) Leaves Extract on Lead Acetate Induced Neurotoxicity in Cerebellum of Adult Wistar Rats. *J. Med. Dent. Sci. Res.* **11**, 36–48 (2024).
80. Almadiy, A. A., Al-Ghamdi, M. S., Al Galil, A. & Dar, S. A. F. M. in *Natural Pesticides and Allelochemicals* 261–278CRC Press, (2025).
81. Gupta, I. et al. Plant essential oils as biopesticides: Applications, mechanisms, innovations, and constraints. *Plants* **12**, 2916 (2023).
82. Nicoletti, M., Murugan, K., Canale, A. & Benelli, G. Neem-borne molecules as eco-friendly control tools against mosquito vectors of economic importance. *Curr. Org. Chem.* **20**, 2681–2689 (2016).
83. Mordue, A. J. & Nisbet, A. J. Azadirachtin from the neem tree *Azadirachta indica*: its action against insects. *Anais da Sociedade Entomológica do Brasil*. **29**, 615–632 (2000).
84. Saleem, S., Muhammad, G., Hussain, M. A. & Bukhari, S. N. A. A comprehensive review of phytochemical profile, bioactives for pharmaceuticals, and pharmacological attributes of *Azadirachta indica*. *Phytother. Res.* **32**, 1241–1272 (2018).
85. Bravo-Arrepol, G. et al. Isolated lignans of *araucaria araucana* (molina) k. Koch provide wood protection against attack by the xylophagous fungus *Pleurotus ostreatus* (jacq.) p. Kumm. *J. Chil. Chem. Soc.* **68**, 5871–5875 (2023).
86. Kurniawanti, A. D., Sugita, P., Suparto, I., Dianhar, H. & Rahayu, D. Bioactive compounds of flavone dimers from Indonesian *Araucaria columnaris* leaves. *Rasayan J. Chem.* **16**, 1872–1882 (2023).
87. Huma, Z. et al. *Azadirachta indica*-based green fabrication of metal oxide nanoparticles: a state-of-the-art review. *Nano Biomed. Eng.* **17**, 373–385 (2025).
88. Jabeen, K., Javaid, A., Ahmad, E. & Athar, M. Antifungal compounds from *Melia azedarach* leaves for management of *Ascochyta rabiei*, the cause of chickpea blight. *Nat. Prod. Res.* **25**, 264–276. https://doi.org/10.1080/14786411003754298 (2011).
89. Li, C. & Seeram, N. P. Ultra-fast liquid chromatography coupled with electrospray ionization time-of-flight mass spectrometry for the rapid phenolic profiling of red maple (*Acer rubrum*) leaves. *J. Sep. Sci.* **41**, 2331–2346. https://doi.org/10.1002/jssc.201800037 (2018).
90. Bystrom, L. M., Lewis, B. A., Brown, D. L., Rodriguez, E. & Obendorf, R. L. Characterization of phenolics by LC-UV/vis, LC-MS/MS and sugars by GC in *Melicoccus bijugatus* Jacq. 'Montgomery' fruits. *Food Chem.* **111**, 1017–1024. https://doi.org/10.1016/j.foodchem.2008.04.058 (2008).
91. Ghareeb, M., Saad, A., Ahmed, W., Refahy, L. & Nasr, S. HPLC-DAD-ESI-MS/MS characterization of bioactive secondary metabolites from *Strelitzia nicolai* leaf extracts and their antioxidant and anticancer activities in vitro. *Pharmacogn. Res.* **10** (2018).
92. Ashraf, H., Moussa, A., Seleem, A., Eldahshan, O. A. & Singab, A. N. UPLC-ESI/MS/MS Profiling and Anti-Inflammatory Activity of *Gleditsia caspica*. *Archives Pharm. Sci. Ain Shams Univ.* **4**, 124–134 (2020).
93. El-Wakil, E. A., Abdel-Hameed, E. S. S., El-Sayed, M. M. & Abdel-Lateef, E. E. Identification of the chemical composition of the methanolic extract of *Salix tetrasperma* Roxb. using LC-ESI-MS and evaluation its potential as antioxidant agent. *development* 1, 2 (2015).
94. Ağalar, H. G., Çiftçi, G. A., Göger, F. & Kırımer, N. Activity guided fractionation of *Arum italicum* Miller tubers and the LC/MS-MS profiles. *Rec Nat. Prod.* **12**, 64–75 (2018).
95. Baz, M. M. et al. Efficacy of Hot *Capsicum annuum* Extracts Against the Biological Activity of *Culex pipiens* and *Musca domestica* Larvae with their Phytochemical Profiles. *Acta Parasitol.* **70**, 1–21 (2025).
96. Elhawary, E. A. et al. Seasonal variation effect on different *Physalis peruviana* L.(Solanaceae) waste extracts and investigation of their efficacy against *Culex pipiens* and Musca domestica. *Sci. Rep.* **15**, 1–22 (2025).
97. Attia, R. A., El-Dahmy, S. I., Abouelenein, D. & Abdel-Ghani, A. E. S. LC-ESI-MS profile, cytotoxic, antioxidant, insecticidal and antimicrobial activities of wild and in vitro propagated *Tanacetum sinaicum* Del. ex DC. *Zagazig J. Pharm. Sci.* **31**, 8–21 (2022).

98. Azevedo, J., Oliveira, J., Cruz, L., Mateus, N. & de Freitas, V. Identification and structural characterization of a novel (+)-catechin-caffeic acid adduct present in wines. *Food Chem.* **442**, 138480 (2024).
99. STĂNILĂ, A. et al. Extraction and characterization of phenolic compounds from rose hip (*Rosa canina* L.) using liquid chromatography coupled with electrospray ionization-mass spectrometry. *Notul. Botan. Horti Agrobotan. Cluj-Napoca*. **43**, 349–354 (2015).
100. Elhawary, E. A., Mostafa, N. M., Labib, R. M. & Singab, A. N. Metabolomic profiles of essential oils from selected *Rosa* varieties and their antimicrobial activities. *Plants* **10**, 1721 (2021).
101. Abdelaziz, S. et al. Ultra performance liquid chromatography-tandem mass spectrometeric analysis of ethyl acetate fraction from Saudi *Lavandula coronopifolia* Poir and evaluation of its cytotoxic and antioxidant activities. *J. Herbmed Pharmacol.* **9**, 268–276 (2020).
102. Irakli, M., Skendi, A., Bouloumpasi, E., Chatzopoulou, P. & Biliaderis, C. G. LC-MS Identification and Quantification of Phenolic Compounds in Solid Residues from the Essential Oil Industry. *Antioxid. (Basel)*. 10. https://doi.org/10.3390/antiox10122016 (2021).
103. Schmeda-Hirschmann, G., Astudillo, L., Rodríguez, J., Theoduloz, C. & Yáñez, T. Gastroprotective effect of the Mapuche crude drug *Araucaria araucana* resin and its main constituents. *J. Ethnopharmacol.* **101**, 271–276 (2005).
104. Patyra, A., Dudek, M. K. & Kiss, A. K. LC-DAD–ESI-MS/MS and NMR Analysis of Conifer Wood Specialized Metabolites. *Cells* **11**, 3332 (2022).

Acknowledgements

This research was funded by the Deanship of Scientific Research and Libraries at Princess Nourah bint Abdulrahman University, through the Research Funding Program, Grant No. (FRP-2025-3)

Author contributions

Conceptualization, LAA, EAE, LAA, AS, MMB; methodology, LAA, EAE, LAA, AS, MMB; validation, LAA, EAE, LAA, AS, MMB; formal analysis, LAA, EAE, LAA, AS, MMB; investigation, LAA, EAE, LAA, HMA, AS, MMB; resources, LAA, EAE, LAA, AS, MMB; data curation, LAA, EAE, LAA, HMA, AS, MMB; writing—original draft preparation, LAA, EAE, LAA, HMA, AS, MMB; writing—review and editing, LAA, EAE, LAA, HMA, AS, MMB; supervision, LAA, EAE, LAA, AS, MMB and; All authors have read and agreed to the published version of the manuscript.

Funding

Not available.

Declarations

Competing interests

The authors declare no competing interests.

Institutional Review Board Statement

The study was conducted according to the guidelines of the Declaration of Benha University and was approved by the Ethics Committee of the Faculty of Science, Benha University (Code: BUFS-REC-2025-478 Ent). The research adhered to all institutional and ethical guidelines for invertebrate studies, ensuring humane treatment of treated insect with minimal suffering and environmental impact, in compliance with approved research ethics standards.

Additional information

Correspondence and requests for materials should be addressed to L.A.A., M.M.B. or A.S.